ARCHIVES OF TRANSPORT *ISSN (print):* *0866-9546*
Volume 75, Issue 3, 2025 ***e-ISSN (online):*** *2300-8830*
DOI: *10.61089/aot2025.dq8tcg20*

A FUZZY LOGIC-BASED CAR-FOLLOWING MODEL FOR SIMULATING TRANSIT VEHICLE MOVEMENT AT AND AROUND BUS STOP USED BY VARIOUS USERS

Justyna Stępień[1]

[1] *Faculty of Civil Engineering and Architecture, Kielce University of Technology, Kielce, Poland*

***Abstract**:*

Linking urban bus transit analysis with traffic engineering contributes to safe and efficient movement of people. A simulation model capable of modelling passenger service at bus stops and traffic conditions around bus stops is an excellent tool in transit efficiency assessment. In the paper, the analysis focused on street segments between intersections with bus stops used by regular bus service, various other transit providers (private operators), and other users (taxis, passenger cars). Large numbers of minibuses of non-urban bus operators stopping at bus stops cause significant disruptions in the traffic flow. The apparent differences in the efficiency and operation of the stops designed for use by local buses and those used by other users required additional analyses. In the probabilistic and simulation models of bus stop operation developed so far, did not use car-following models for the modelling of the movement of buses and other vehicles at and in proximity of bus stops. This theory is used in off-the-shelf traffic microsimulation software packages, but they do not allow a reliable representation of how bus stops operate under the deregulated service of passengers (oversaturated bus stops with a variable number of service channels). This study analyses the movement of buses and other vehicles at a bus stop area using a car-following model with fuzzy logic applied for parameter estimation. A microscopic simulation model was built and tested. The selection of the shape of fuzzy sets and membership functions was based on multiple simulation runs. The model simulates queuing and delays imparted on buses and traffic flow in lanes adjacent to bus stops used by city buses and other transit providers. The simulation results were compared with the real-world processes with the use of the author's two-stage method. Verification based on the PROC and SDDIST indicators showed that the simulated and observed distributions of travel time and delay were highly consistent, with maximum deviations below approximately 10%. The analysis also confirmed that the model accurately reproduces average delays caused by bus queues and vehicle interactions near shared-use stops. The analyses demonstrated that the fuzzy logic-based car-following model proposed in this study is suitable for planning, designing, and relocating urban bus stops used by various operators. The feasibility of the developed model and directions of its further development were evaluated.

Keywords: *urban bus stop, computer simulation, car-following model, fuzzy-logic based model, various bus operators*

To cite this article:

Stępień, J., (2025). A fuzzy logic-based car-following model for simulating transit vehicle movement at and around bus stop used by various users. Archives of Transport, 75(3), 93-140. https://doi.org/10.61089/aot2025.dq8tcg20

Contact:
1) justynas@tu.kielce.pl [https://orcid.org/0000-0002-9663-0191] – corresponding author

1. Introduction

Increasing congestion and limited road capacity in European cities have made the optimisation of public transport operations one of the key challenges in urban traffic engineering. Bus transport, as the most flexible and widely used form of public transport, plays a crucial role in maintaining accessibility and ensuring continuity of passenger flow. The efficiency of bus stop operation and the traffic flow around them can be quantified by modelling the movement of buses and other vehicles within and near stop areas, including adjacent lanes. Due to the complexity and stochastic nature of these processes, microscopic simulation models are required to describe them with sufficient accuracy. Linking the analysis of bus transit operation with traffic engineering contributes to the development of safe and efficient passenger movement (Bauer, Dźwigoń, and Richter 2021; Cingel, Drliciak, and Celko 2021), network-level modelling (Drabicki, Islam, and Szarata 2021; Faron 2018), and rational infrastructure design (Phillips, Hagen, and Berge 2021; Śleszyński et al. 2023), as well as the design of adequate pavement structures (Chomicz-Kowalska and Stępień 2016; Lee and Le 2023).

At the European level, strategic frameworks such as (The New EU Urban Mobility Framework 2021), the (Sustainable and Smart Mobility Strategy – Putting European Transport on Track for the Future 2020), and (Guidelines for Developing and Implementing a Sustainable Urban Mobility Plan 2019) underline the need to improve the punctuality and reliability of bus transport services. These documents highlight the importance of reducing operational delays at bus stops, which represent a substantial portion of total travel time. Proper analytical and simulation models of stop operation provide the technical basis for assessing capacity, determining the number of berths, and evaluating traffic conditions in the area of stops.

In Central and Eastern European (CEE) countries such as Poland, the Czech Republic, Slovakia, Romania, Hungary, and the Baltic States, bus transport continues to play a dominant role in both urban and regional mobility. The economic transformation and deregulation of the transport sector during the 1990s led to the development of mixed systems operated by urban, regional, and private operators (Fitzová and Matulová 2020; Pojani and Stead 2015; Taylor and Ciechański 2018). This process has resulted in a high differentiation of organisational structures and service standards (Hansson et al. 2019). As a consequence, many cities now operate shared-use bus stops, where vehicles from various operators—urban, suburban, private regional operators and long-distance buses—use the same infrastructure in an uncoordinated manner. Furthermore, such stops are frequently accessed by taxis and private vehicles, which increases the heterogeneity of vehicle interactions and passenger flows. The irregular use of the stop area generates variable dwell times, dynamic spacing between vehicles, and localised traffic disruptions. Figure 1 presents an example of a shared-use bus stop located on an urban arterial road, used by various operators and other users. The shared use of this infrastructure results in randomly selected bus stopping positions, increased variability in dwell time, and potential disturbances to traffic flow in adjacent lanes. Figure 1 illustrates the selected types of traffic disurbances identified within the analysed bus stop areas:

- D1 – additional stop of a vehicle in traffic lanes adjacent to the bus stop,
- D2 – reduction of vehicle speed in traffic lanes adjacent to the bus stop,
- D3 – delayed start of a queued vehicle in lanes adjacent to the bus stop,
- D4 – additional stop of taxis and other vehicles in the traffic lane with the bus stop,
- D5 – additional stop for buses and other vehicles in the approach of the intersection before the bus stop,
- D6 – blocking of a bus from entering the passenger service berth and related overtaking manoeuvres,
- D7 – blocking of a bus from leaving the passenger service berth and related overtaking manoeuvres,
- D8 – passenger service conducted irregularly, outside the designated boarding and alighting area,
- D9 – passenger service performed at a large distance from the preceding vehicle,
- D10 – blocking of a side-street entry at the intersection located before the bus stop,
- D11 – traffic weaving within the bus stop area (lane changes related to turning movements at the adjacent intersection).

Traffic disruptions that occur at and around shared use bus stops are associated with additional time losses experienced by buses due to queueing and limited opportunities to merge into the traffic stream, as well as with secondary delays affecting vehicles in adjacent lanes. The average delays and the probability of bus queuing represent measures of the practical capacity and service level of the stop, while the average delay and mean speed of vehicles in adjacent lanes determine the overall efficiency and capacity of the road section or intersection.

Shared-use bus stops, where multiple types of operators and other users interact dynamically, introduce significant complexity into local traffic conditions. These interactions generate stochastic patterns of vehicle movement, irregular passenger service, and unpredictable lane usage. Considering these conditions, the main objective of this study is to develop and verify a microscopic simulation model that describes vehicle movement and passenger service at shared-use urban bus stops. The proposed model integrates fuzzy logic-based car-following rules with probabilistic sub-models of passenger service, vehicle movement in adjacent lanes, and lane-changing. Its purpose is to assess the operational efficiency and traffic disturbances resulting from irregular and heterogeneous bus stops by multiple operators. The main contribution of this research lies in integrating fuzzy logic-based car-following behaviour with probabilistic passenger service representation, enabling the realistic simulation of heterogeneous and irregular bus stop operations under urban traffic conditions.

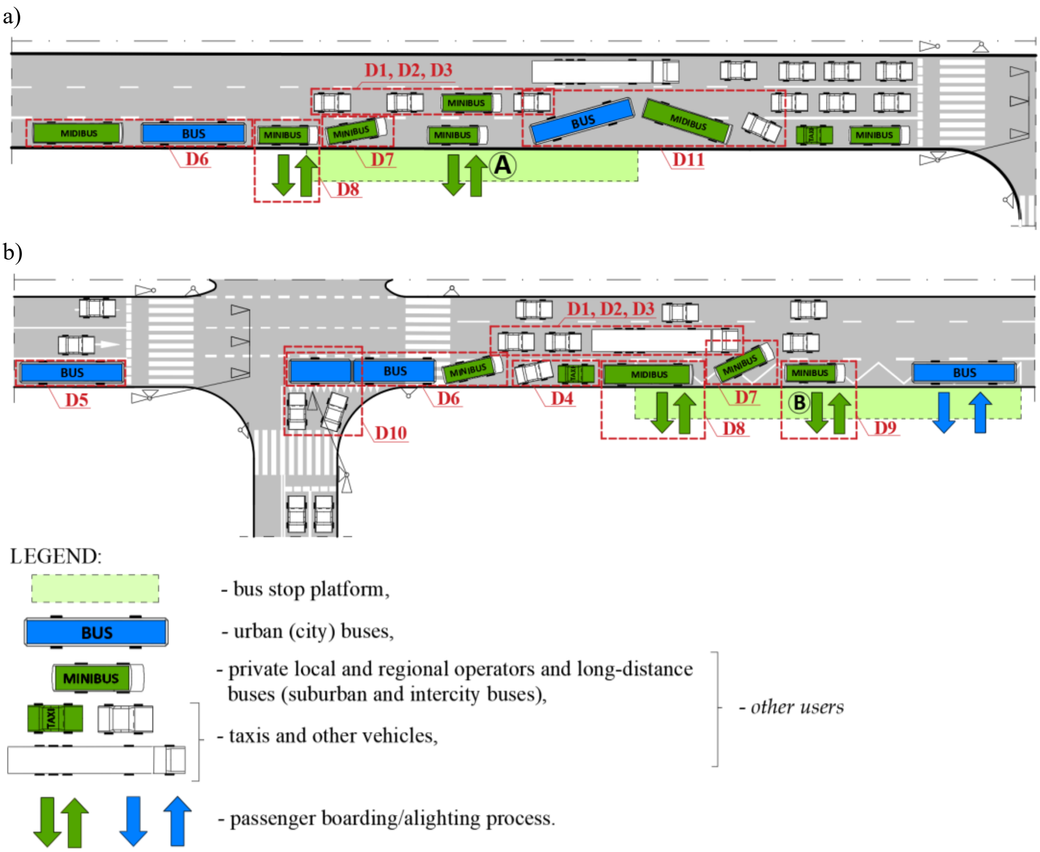

Fig. 1. Example of traffic disturbances in the bus stop area used by various operators: a) at the intersection entry, b) at the intersection exit

2. Literature review

2.1. Car-following models and fuzzy-logic-based approaches

Car-following behaviour significantly influences driving safety and traffic flow stability. Thus, the car-following theory is one of the basic of traffic flow theories using traditional numerical models and artificial intelligence (AI). The most common vehicle movement simulation models include the car-following models classified as Ghazis - Herman - Rothery models (GHR models) proposed in 1958 by the General Motors laboratory in Detroit (Chandler, Herman, and Montroll 1958), collision-avoidance (cellular automata CA) models (Benekohal & Treiterer, 1988; Gipps, 1981; Tian, 2012), linear models, psychophysical models or the AP (action-point) model (Fritzsche 1994), fuzzy logic-based models (Chakroborty and Kikuchi 2003; Takagi and Sugeno 1985), neural-fuzzy models (Khodayari et al. 2012; X. Ma 2006) and neural network based model (Xu, Ma, and Wang 2022). Deep learning algorithm has been increasingly applied in car-following behaviour (J. Liu et al. 2023; L. Ma and Qu 2020; Mo, Shi, and Di 2021; X. Wang et al. 2019; Xu, Ma, and Wang 2022). Autonomous driving control algorithms have developed car-following modules (Ahmed, Huang, and Lu 2021; Z. Wang et al. 2022). Many traffic simulation tools (such as Vissim, Aimsum etc.) also use the car-following and lane changing theory (Ištoka Otković et al. 2023; Naghawi, Shattal, and Idewu 2019).

Many researchers used spatial microsimulation methods but did not consider the impacts of bus stops on traffic flow. Researchers (van Hinsbergen et al. 2015) used a Bayesian framework for calibrating and comparing car-following models. Ngoduy and Li (2021) established a general bifurcation structure of a car-following model with multiple delays. Jin et al. (2019) developed an extended link-node structured two-lane cell transmission model (CTM) capable of dynamically capturing the effect of lane blockage at bus stops and comprehensively modelling mandatory and discretionary lane change (MLC & DLC) manoeuvres along a bus route under various levels of traffic demand.

In Poland, Krystek (1980) applied the car-following theory to simulate vehicle traffic in a multi-lane one-way road section between intersections. In an attempt to improve the efficiency of traffic lights at intersections, they analysed the disturbance in the movement of one vehicle resulting from the speed change of another vehicle. The model (Krystek 1980) did not take into account bus stops or bus lanes.

Further developments in car-following modelling aimed to address the variability of driver behaviour and the uncertainty of decision processes. The work by Zheng & McDonald (2005) was among the first to employ fuzzy inference systems for car-following, introducing rule-based reasoning reflecting linguistic variables such as “small gap” or “high relative speed”. Similarly, Chakroborty & Kikuchi (2003) proposed a calibration method for fuzzy membership functions using empirical car-following data, which demonstrated the flexibility of fuzzy logic in representing driver heterogeneity. Khodayari et al. (2012) advanced this line by integrating neural networks with fuzzy logic, forming a neuro-fuzzy model capable of learning driver reactions dynamically.

Hybrid models have also evolved with the inclusion of adaptive learning mechanisms (Feng et al. 2019; X. Ma 2006), human-like decision structures (Feng, Iravani, and Brace 2021), and heterogeneity-aware formulations for mixed traffic (Zhu et al. 2024). Sangole and Patil (2014) applied ANFIS to model gap-acceptance behaviour in heterogeneous conditions, confirming the potential of neuro-fuzzy inference for complex urban interactions. Despite these advances, most studies have focused on homogeneous highway or urban stream scenarios rather than constrained and irregular flow near bus stops.

Recent deep-learning-based and physics-informed approaches (J. Liu et al. 2023; X. Wang et al. 2019) achieve remarkable predictive accuracy but sacrifice interpretability. In contrast, fuzzy logic and neuro-fuzzy systems retain a transparent rule structure, making them suitable for integration into traffic microsimulation models that require both realism and interpretability.

The fuzzy theory successfully found applications in the wide range of subject fields, including traffic engineering and bus transit analyses. The fuzzy logic traffic system was analysed for signalised intersections with the use of computer simulation (Tunc, Yesilyurt, and Soylemez 2021; Vatchova, Boneva, and Gegov 2023) and other methods based on deep Q learning (Tunc and Soylemez 2023). Fuzzy logic-based methodology was also used for the quantification of the level of traffic congestion in study (Toan and Wong 2021), but only on highways, not for urban conditions. Fuzzy logic-based transit priority strategy was proposed in study (Jovanović and Teodorović 2022) and implemented in a Vissim environment, but did not take into account bus stops. In the paper (Milla et al. 2012) was proposed a control scheme was proposed for the operation of a bus system running along a linear corridor, based on expert rules and fuzzy logic. The study focused on headway regulation and did not include microscopic passenger processes or mixed-traffic interactions at and around the bus stop used by various users.

2.2. Bus stop simulation models

Early Polish studies, including Rudnicki (Rudnicki 1977), presented one of the first stochastic microsimulation approaches to modelling the functioning of a bus stop, focussing on the probabilistic nature of passenger service and bus arrival processes. Later, Bąk (2010) extended this concept by modelling queues of buses and passenger exchange processes using deterministic service rules and fixed berth lengths. These works established the foundation for bus stop efficiency analysis in microscopic frameworks.

An extended car-following model was proposed considering the influence of bus in the study (Jinxing et al. 2017), but only for single lane traffic on the highway. This model discriminates four types of car-bus following combination. In the model developed by Fernández (2010), the process of bus re-entering the traffic in the adjacent lane is based on the gap-acceptance model. Wang et al. (2019) developed a model incorporating a diffusion approximation method to study the correlation between bus stop failure rate and bus stop operation. Using kinematic wave theory, (Gu et al. 2013) built a model to determine the position of a bus stop at the entry of an intersection with traffic lights, taking into account basic efficiency measures, such as vehicle delays and queues. Alonso et al. (2013) presented a microscopic simulation model of bus stop operation developed specifically for Spanish conditions. The model included stops with one to three passenger boarding/alighting points based on the FIFO rule (First In, First Out). Joyce and Jagar (1990) analysed the impact of stops on the traffic flow based on a computer simulation using the TRANSYT method.

Long bus queues are often observed at the most congested stops during peak periods. The impacts of bus overtaking policies on bus stops was analysed in studies (Hu, Shen and Gu 2023; L. Liu, Bian, and Nie 2022). Other papers related to the operation of bus stops incl. ((Edward) Kim, Levy, and Schonfeld 2019; Adamski 1992; Berrebi, Watkins, and Laval 2015; Meng and Qu 2013; Shen et al. 2019; Tirachini, Hensher, and Rose 2014) do not allow a reliable representation of how bus stops operate under the deregulated service caused by regional bus operators (suburban and interurban) with a variable number of service channels. In the study, the impact of the bus stop near the signalised intersection on the traffic flow from two aspects, traffic volume and delay, was analysed using the theory of car -following and lane changing theory was analysed in study (Zhenyu and Meiying 2019). The impact of bus stops and other factors on traffic flow was also investigated in other studies (Carrillo-González et al. 2021; Jin et al. 2022; Raj, Asaithambi, and Ravi Shankar 2022).

Further microsimulation research has expanded the understanding of passenger processes at stops. For example, Xue et al. (2022) used simulation-based and cellular automata approaches, respectively, to evaluate bus dwell times and passenger interactions. Studies (Kwesiga, Guin, and Hunter 2025; T. Wang et al. 2024) further incorporated stochastic process models and automatic passenger count (APC) data to analyse dwell time variability and its effects on capacity and signal priority. These studies highlight the importance of stochastic representation in modelling passenger service processes. However, they generally neglect mixed-traffic interactions and the dynamic spatial variability of stopping positions typical for shared-use bus stops.

Many of the probabilistic and simulation models of bus stop operation did not use car-following models for modelling of the movement of buses and other vehicles at and in proximity of bus stops. This theory is used in standard traffic microsimulation software packages, but they do not allow a reliable representation of how bus stops operate under the deregulated service of passengers (with a variable number of service channels).

Despite these developments, most existing models assume uniform vehicle dimensions, fixed berth use, and deterministic service rules. Such simplifications do not reflect the actual conditions at shared-use stops, where buses belonging to different operators (urban, regional, intercity, and private) and even taxis use the same space, resulting in irregular headways, variable stopping positions, and frequent traffic disruptions. The probabilistic representation of these processes is essential. Empirical observations show that buses often choose stopping positions based on passenger clusters along the platform, creating large inter-vehicle gaps and nonsequential service orders. Therefore, in the proposed model, both vehicle movement and passenger service are represented probabilistically. Bus dwell times, arrival patterns, and passenger interactions are simulated using random variables derived from measured data, while surrounding traffic follows fuzzy-logic-based car-following and lane-changing models. This combination allows for realistic reproduction of the dynamic and irregular behaviour observed at shared-use urban stops. Such an integrated approach bridges the methodological gap between existing bus-stop simulation frameworks and traffic flow models, linking probabilistic passenger service, heterogeneous vehicle interactions, and fuzzy rule-based movement logic.

2.3. Comparison of the state of the research and the scope of present study

The analysis in this paper focusses on street segments between intersections containing bus stops used by multiple operators and other vehicles (taxis, passenger cars, trucks). The apparent differences in the operation of stops serving various providers required additional analyses. Given the purpose of the study, a microscopic modelling approach was adopted, allowing a detailed examination of vehicle interactions, particularly between departing buses and surrounding traffic. Initial attempts using commercial software such as Vissim (PTV Group, 2025) proved insufficient, as the program's fixed berth allocation and deterministic service rules failed to reproduce the irregular stop usage observed under field conditions. Therefore, an original fuzzy logic–based simulation model was developed, integrating the probabilistic variability of vehicle interactions with behavioural decision rules. The model enables realistic analysis of car-following, lane changing, and multi-berth stop operation under probabilistic, heterogeneous traffic conditions.

To position the developed model within the current state of knowledge, a literature review was performed. Table 1 summarises the most relevant car-following and fuzzy-logic-based models, illustrating the methodological evolution from deterministic to probabilistic and hybrid approaches, as well as the increasing attention to mixed- and shared-use urban traffic environments. Additional references are provided in Appendix A (Table A.1).

Table 2 provides a comparative summary of the most representative microscopic models of bus stop operation, focussing on their methodological approaches, assumptions, and applicability to heterogeneous and shared-use urban traffic conditions. The table emphasises the differences between deterministic and probabilistic frameworks and highlights the limited integration between bus stop operation models and car-following theory. Additional references supporting this analysis are included in Appendix A (Table A.2).

The comparative analysis presented in Tables 1, 2, A1 and A2 (Appendix A) shows that microscopic traffic models and bus stop operation models have evolved in parallel but rarely overlap in their methodological scope. Deterministic and psycho-physical car-following models (e.g., Bando et al. 1995; Fritzsche 1994; Gipps 1981) provided the basis for understanding vehicle interactions, while fuzzy-logic-based and hybrid models (e.g., Chakroborty and Kikuchi 2003; Feng et al. 2019; Feng, Iravani, and Brace 2021; Khodayari et al. 2011, 2012; L. Li, Yang, and Cao 2014) introduced behavioural flexibility and uncertainty representation. However, these approaches typically focus on homogeneous traffic flows and do not incorporate bus stop operations or stochastic disturbances caused by passenger service. It is also noteworthy that most existing car-following and fuzzy-logic models were developed for highway or general traffic conditions, (e.g., Bando et al. 1995; Gipps 1981; Khodayari et al. 2011; Zheng and McDonald 2005). Only a few recent studies, for example (Feng et al. 2019; Zhu et al. 2024) explicitly address urban and heterogeneous traffic environments, which are essential for analysing shared-use bus stop operation. On the contrary, microsimulation models of bus stop operation (e.g., Bąk 2010; Fernández 2010; Gu et al. 2013; Tian 2012; T. Wang et al. 2024; Xue et al. 2022) concentrate on boarding and alighting processes, vehicle queueing, or bus dwell times. Most of them adopt deterministic service rules (FIFO or fixed-berth assignment), assume a homogeneous fleet, and neglect irregular vehicle–passenger interactions or dynamic stopping positions.

Table 1. Comparison of key car-following models, fuzzy-logic-based approaches, and simulation tools (CF – car-following, PT - public transport, AV - autonomous vehicle, ANFIS - adaptive neuro-fuzzy inference system)

Model/study	Method/ approach/data source	Application context	Advantages	Limitations	Relevance to bus or stop operation
Krystek (1980)	Microscopic simulation based on car-following theory (analytical and empirical traffic data)	Multilane urban and interurban road segments	Early Polish CF model; interpretable behavioural parameters	No PT or bus stop modelling	Partial – traffic near stops, no passenger processes
Gipps (1981)	Deterministic car-following model (analytical)	General traffic flow	Simplicity, broad applicability	Lacks behavioural variability	No – general traffic only
Bando et al. (1995)	Optimal Velocity Model (simulation)	Highway traffic	Theoretical clarity	Unrealistic driver response	No – general traffic only
Chakroborty and Kikuchi (2003)	Fuzzy inference system; calibration of membership functions (field trajectories)	Car-following	Interpretability, rule-based logic	Limited dataset	Partial – urban traffic only
Zheng and McDonald (2005)	Classical fuzzy inference system (simulation)	Highway CF	Transparent rule structure	Motorway observations; limited field calibration of fuzzy rules	No – general traffic
Khodayari et al. (2011)	Improved predictive fuzzy model	Experimental data	Smooth transitions, higher accuracy	No analysis for mixed traffic	Partial – urban driving only
Khodayari et al. (2012)	Neural network-based fuzzy driver model (experimental)	General CF	High prediction accuracy	Limited transparency of the decision structure	Partial – urban freeway only
Jinxing et al. (2017)	Extended CF model including bus influence (simulation)	Mixed traffic with buses	Incorporates bus effects	Freeway-only context	Yes – bus following model
C. Wang et al. (2019)	Reinforcement learning for autonomous CF (simulation)	AV platoons	Adaptive control	No human behaviour modelling	No – general CF model
Feng et al. (2019)	ANFIS with real driving data	On-road trajectories	Driver-type adaptation	Limited interpretability	Partial – urban driving only
Feng, Iravani, and Brace (2021)	Human-like fuzzy driver model (naturalistic data)	Lane keeping and CF	Human decision-making	Complex rule structure	Partial – behavioural logic only
Zhu et al. (2024)	Heterogeneity-Aware CF Model (simulation data)	Mixed vehicle traffic flow	Considers vehicle type diversity and adaptive response	Not fuzzy-based, but physics-driven; No passenger layer	Partial – heterogeneous traffic
PTV Vissim (PTV Group 2025)	Commercial microsimulation software with CF, lane-changing and PT modules	Urban traffic and bus stops	Widely applied, validated tool for traffic and PT analysis	Fixed service rules and stop geometry; limited stochasticity	Partial – models bus stops, but not irregular shared-use operation
Present study	Fuzzy logic-based car-following with probabilistic parameter generation	Urban shared-use bus stops	Combines fuzzy CF rules with probabilistic parameters; realistic mixed-traffic simulation	Requires detailed calibration and computational resources	Yes – integrates bus stop operation with surrounding traffic flow

Table 2. Comparison of key microscopic simulation models of bus stop operation and their relevance to shared-use, unregulated passenger service conditions (CF - car-following, PT-public transport)

Model/study	Method/ approach/data source	Application context	Advantages	Limitations	Relevance to this study
Rudnicki (1977)	Early discrete-event and stochastic simulation of bus-stop operation (analytical and empirical parameters)	Urban bus stops	One of the first stochastic microlevel simulations of stop operation; foundation for Polish and European research	Simplified buses–traffic interaction; static infrastructure	Historical and methodological reference – early stochastic modelling of bus-stop processes forming conceptual basis for later probabilistic models
Fernández (2010)	Microscopic simulation of bus-stop operation using analytical and simulation data	Urban bus stops	Canonical detailed model of bus dwell and queueing; basis for later microsimulations	Simplified passenger interactions	Fundamental reference for stochastic bus-stop modelling
Bąk (2010)	Microscopic simulation of bus service process at stop; analysis of queues and service rules	Urban bus stop operation (service area)	Examines boarding–alighting service and bus queue formation with constant number of berths	Fixed service rule; equal berth lengths; no surrounding traffic	Reference for structured, regulated bus-stop operation — contrasted with dynamic shared-use model
Gu, Cassidy, and Li (2015)	Analytical queueing model of bus operations at curbside stops (Markov/steady state)	Urban curbside stops	Clear estimates of bus delay and required berths	Assumes ordered service; homogeneous fleet	Queueing benchmark for probabilistic service component
J. Zhang et al. (2018)	Field study and comparative analysis of bus stop designs (four geometric types)	Urban bus stops	Empirical comparison of bus stop layouts and bus/bike interaction effects	Focus on low traffic density; no microscopic passenger simulation	Reinforces impact of stop geometry and bus dwelling on traffic disruptions
Krivda et al. (2021)	Vissim/Viswalk microsimulation of public-transport node (stops and pedestrians)	Urban hub	Demonstrates multimodal microsimulation workflow	Fixed modules; deterministic rules	Confirms limits of commercial tools
L. Liu, Bian, and Nie (2022)	Simulation of bus overtaking and queue rules at multi-line stops	Urban bus terminals	Defines service order and overtaking logic	Fixed, ordered service	Contrast to unregulated shared-use operation
T. Wang et al. (2024)	A stochastic process approach in bus dwell estimation and overtaking manoeuvres	Urban stops under mixed traffic	Stochastic modelling of dwell and overtaking; empirical validation	Does not consider passenger heterogeneity	Methodologically close to the stochastic component of this study
Vissim (PTV Group 2025)	Commercial microsimulation software (traffic and PT module)	Urban roads and bus stops	Advanced visualization and empirical validation	Fixed service rules; limited variability	Reference simulation environment
Present study	Fuzzy-logic-based model of vehicle movement and probabilistic passenger service (video data)	Urban shared-use bus stops with unregulated service and heterogeneous fleet	Dynamic vehicle stopping position choice; passenger-by-passenger and vehicle-by-vehicle modelling; probabilistic distributions; multi-operator service; traffic and passenger disturbances	High computational complexity; requires detailed field calibration	Novel approach – integrates probabilistic passenger dispersion, unregulated service, heterogeneous fleet, and fuzzy CF modelling into a unified microsimulation framework

Tian (2012) represents an early attempt to integrate bus stop processes with adjacent traffic flow using cellular automata simulation, yet without probabilistic service or fuzzy decision logic. Similarly, Wang et al. (2024) incorporated stochastic dwell-time estimation, but the surrounding vehicle interactions were treated deterministically. To date, no existing study has explicitly coupled a probabilistic or fuzzy car-following framework with a stochastic passenger service model to capture the mutual interdependence of stop operation and adjacent traffic dynamics. Therefore, the main research gap identified is the absence of a microscopic, behaviourally interpretable model that simultaneously represents:

– fuzzy logic-based vehicle interactions (car-following and lane changing),
– probabilistic passenger service and dynamic vehicle stopping positions,
– heterogeneous vehicle fleets (urban, suburban, intercity buses, taxis, private cars), and
– local traffic disturbances due to irregular stop operations.

Many of the cited studies, particularly those conducted in Asian metropolitan contexts, developed under traffic and geometric conditions from those observed in Central European cities. Therefore, their findings cannot be directly transferred to European conditions without adjustment for local operational and behavioural factors.

The novelty of the proposed model lies in bridging these two modelling domains by integrating a fuzzy-logic-based vehicle movement framework with probabilistic passenger service and dynamic stop usage. This enables microscale simulation of shared-use bus stops under the conditions of probabilistic boarding and alighting, random vehicle headways, and spatially dispersed passenger demand. The model thus offers a comprehensive tool for analysing both traffic-flow disruptions and service-process variability in complex urban environments.

In methodological terms, the proposed simulation framework constitutes an extension and integration of the classical Polish models developed by (Bąk 2010; Rudnicki 1977) and (Krystek 1980). It combines their complementary concepts of bus stop operation, passenger service processes, and traffic flow theory into a unified probabilistic–fuzzy microsimulation environment.

Based on the state-of-the-art presented, the objective of this study is to fill the identified research gap by developing a microscopic fuzzy logic-based simulation model that captures vehicle–passenger interactions and the probabilistic nature of the operation of shared-use bus stops under urban traffic conditions.

3. Methodology and scope of analyses

The model was developed using a Python programming language and was based on the measurement data collected using a video filming technique at bus stops in Kielce (KIEL-01÷10) and Kraków (KRAK-01÷091) (Poland) and in adjacent areas with 33 intersections. A total of 118,000 vehicle passes (including about 7 000 buses) at all bus stops and 400, 000 events (including passes through specified sections and stops) were recorded. Average hourly service rates of urban buses stopping for passenger service ranged from 12 bus/h to 50 bus/h. The rates of private local and regional operators and long-distance bus/coach services (PKS) averaged 18 bus/h to 84 bus/h. Taxis and other vehicles (delivery vans, passenger cars, emergency vehicles) also made a stop at the bus stops (up to 11 veh/h). Some of the stops were located on public lanes, leading to heavy traffic not related to the bus stop (maximum 217 veh/h). In other cases, traffic volume rates reached 74 veh/h.

The primary objective was to model the movement of interacting vehicles in terms of lane changing, stopping at the stop, re-entering the traffic stream after passenger service, and traffic lights effect on the movement of buses and other vehicles. The first assumption for the algorithm was that dynamic parameters should simulate the manoeuvres of buses (stopping at and resuming movement from a bus stop) and the movement of other vehicles. The model was designed to be simple, easy to modify and suitable for evaluating traffic conditions on a one-way, multi-lane street segment between intersections. Predicted stopping of a bus at the bus stop and driver's reactions to traffic lights, are included in the model, as is a simplified lane-change algorithm to account for traffic conditions on adjacent lanes.

Figure 2 shows a schematic representation of the system of processes.

Both the adopted assumptions and the form of data (direct measurements by video recording with a reading accuracy of 0.1 s) decided a fuzzy logic approach.

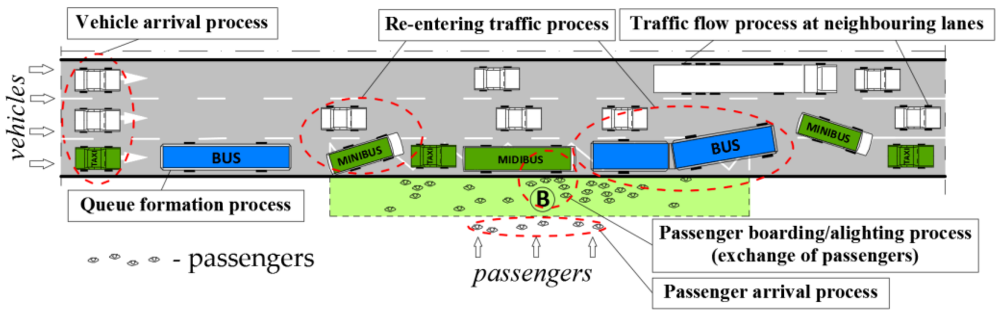

Fig. 2. Basic processes related to bus stop operation

Fuzzy logic controls the vehicle's behaviour relative to other vehicles by regulating a given vehicle's acceleration according to its speed and that of the leading vehicle and distance separating the two vehicles. A significant advantage of this method is that it is not associated with any specific relationship pattern as the relation sought is approximated using fuzzy sets Kosko (1994). For this reason, it is not necessary to choose one specific model from a number of models proposed in the literature, for example, in (Panwai and Dia 2005).
Fuzzy implication has the form:

$$\text{IF } (x_1 \text{ is } A_1) \text{ and}|\text{or } (x_2 \text{ is } A_2) \text{and}|\text{or } \ldots (x_n \text{ is } A_n) \text{ THEN } y = g(x_1, \ldots, x_n) \quad (1)$$

where x_i are the input variables, A_i are the corresponding fuzzy sets, and y_i are the output variables (input variable function). Examples of fuzzy sets in system modelling are provided by Takagi and Sugeno (1985).
The model development and preliminary testing phase involved selecting basic parameters to characterise vehicle movement within a bus stop area. Since the objective was to analyse only the movement of buses and other vehicles, the component for simulating multiple-berth passenger service process was not included in the model. The passenger boarding/alighting process was not included at this stage due to its high randomness which would hinder the interpretation of simulation results and selection of dynamic vehicle parameters. In the simulations, passenger service was represented by the values of passenger exchange times loaded directly from the database of real-world data. In the model, the instants of the vehicle appearance in the simulation were entered directly from the created measurement dataset.

The analysed road segments had geometrical parameters as described in Figure 3. The control area was defined by the cross-sections in which the passage of subsequent vehicles was recorded.
The traffic flow in the model was represented by a series of vehicles described by selected events entered from the measurement datasets. The parameters assigned to them included vehicle type, operator type, lane in which the vehicle appears in the analysed area, time of vehicle appearance, instantaneous speed of the vehicle at the time of entry into the control area, information about lane change, and waiting time/dwell time at the bus stop.

4. Fuzzy logic-based car-following model for vehicle movement simulation

4.1. Test simulations and selection of fuzzy set shapes and membership functions

The basis for the choice of the fuzzy set shape and functions to characterize them was multiple simulation runs based on the measurement data collected at the test sites. The computer program for traffic flow simulation was developed in Python and operated on the principle of successive time instants. A value of *dt* = 0.2 s was adopted as the constant time step for which vehicle traffic was tracked. In the program structure, a separate list of objects was entered for each lane, sorted by the instants of event occurrence in the controlled area within the bus stop. Individual vehicles were the objects with assigned parameters entered from previously developed real world event databases using Python libraries. Then the data was transformed using the established classes. Python is an object-oriented programming language and can be successfully used as a tool to model the movement of buses and other vehicles as objects.

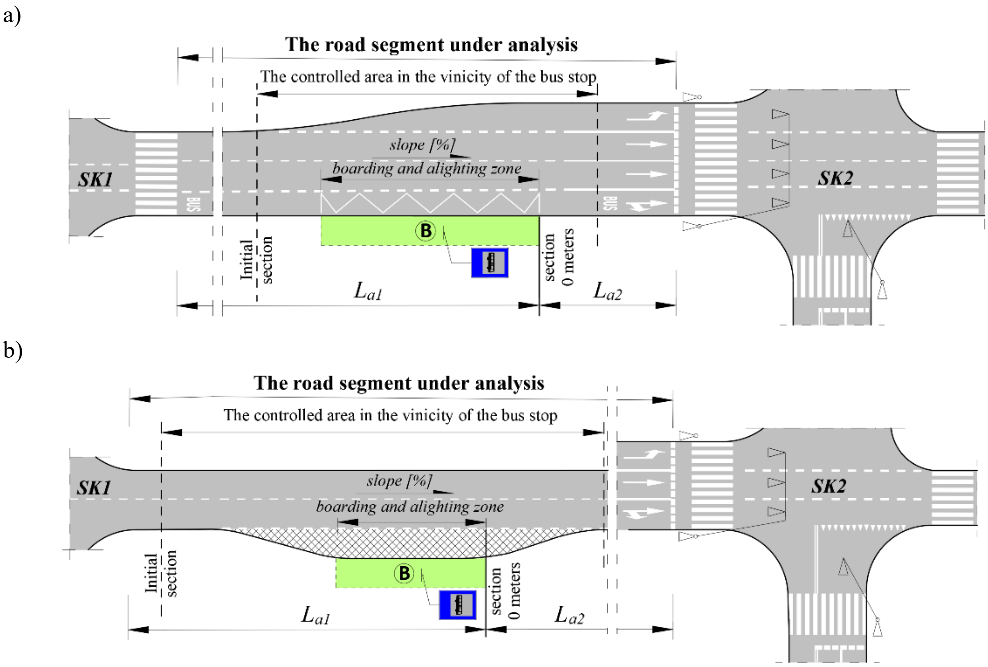

Fig. 3. Examples of analysed road segments between intersections: a) with a stop on the curb lane (bus lane), b) with a stop in a designated bus bay

Three basic groups of vehicles were separated in the model: passenger cars, trucks, and buses. The characteristic dynamic parameters assigned to them were acceleration, delay and maximum speed. The vehicle length depended on the type of the bus and make of individual vehicles (data loaded directly from the dataset). Other parameters for each vehicle movement were established on the spot during simulations according to the movement of other vehicles analysed using fuzzy logic rules. Since one of the assumptions was that buses must respond to the designated stopping point at the bus stop, an additional variable *z*, was introduced to define the distance of the vehicle from the stopping point.

The driver's actions were assumed to fall into one of three movement states, i.e., *maintain speed (following), reduce speed (decelerate), increase speed (accelerate).* In addition, in the absence of a vehicle in front and other factors limiting its movement (e.g. traffic lights, a need to stop at the bus stop), the vehicle could move freely (free flow) at a desired speed. At that stage of model testing, the desired speed was the permitted speed.

It was assumed that at any time instant *t* of vehicle *n* moving (following) on the street section at/around a bus stop, speed $v_n(t)$ is a function of the values of the following parameters referring to the earlier time instant $(t-1)$:

- $v_n(t-1)$ – the speed of vehicle *n* (m/s),
- $v_{n-1}(t-1)$ – the speed of vehicle immediately in front $(n-1)$ (m/s),
- $d(t-1)$ – the distance between the front edge of vehicle *n* and the vehicle immediately in front $(n-1)$ (m),
- $z(t-1)$ – the distance between the front edge of vehicle *n* and the stopping position at the bus stop (m),
- $d_1(t-1)$ – the distance between the front edge of vehicle *n* and the stop line marked with horizontal marking at signalized intersection entry or the distance from the stopping position at the intersection entry (m).

Figure 4 illustrates the parameters of the model. The acceleration of vehicle *n* for a random instant *t* ($a_n(t)$) was assumed to be characterized in fuzzy logic by two variables:

- δv (*t* – 1) – the speed difference between vehicle *n* and the vehicle immediately in front (*n* – 1) (m/s),
- *d* (*t* – 1) – the distance between vehicle *n* and the vehicle immediately in front (*n* – 1) (m).

The space of these variables was divided into three fuzzy subsets. For the speed difference δv, these would be sets meaning that vehicle *n*:

- is approaching (set A_1) – must adjust its speed to the lower speed of the vehicle immediately in front (the leading vehicle) *n*,
- is driving away (set A_2) – moving at a lower speed than the vehicle immediately in front *n*),
- is following (set A_3) – the speed difference between vehicles *n* and (*n* – 1) oscillates around zero, the driver maintains approximately constant safety clearance.

The following sets were determined for distance *d*:

- close (set B_1),
- far away (set B_2),
- at an optimal distance (set B_3).

Acceleration at a given time is defined by the following output functions that provide speed changes δv and distance changes *d* between the vehicles with driver's responses being:

- brake,
- brake rapidly,
- maintain speed,
- accelerate,
- accelerate rapidly.

The algorithm is characterized by the implications given below. These are all possible combinations of three states describing the distance from the vehicle immediately in front *d* and three states describing the difference in speed between vehicles δv.

A reaction to δv and *d* is expressed as an acceleration value defined using the following rules:

- IF *d* IS closing THEN brake rapidly.
- IF *d* IS close AND δv IS following THEN brake.
- IF *d* IS close AND δv IS moving away THEN maintain speed.
- IF *d* IS optimal AND δv IS closing THEN brake.
- IF *d* IS optimal AND δv IS following THEN maintain speed.
- IF *d* IS optimal AND δv IS moving away THEN accelerate.
- IF *d* IS far away AND δv IS closing THEN maintain speed.
- IF *d* IS far away AND δv IS following THEN accelerate.
- IF *d* IS far away AND δv IS moving away THEN accelerate rapidly.

The fuzzy set *stopping*, corresponding to the space of this variable, was described by the Gaussian curve.

A reaction to the distance from the stopping position was determined using an additional rule:

- IF *z* IS stopping THEN brake.

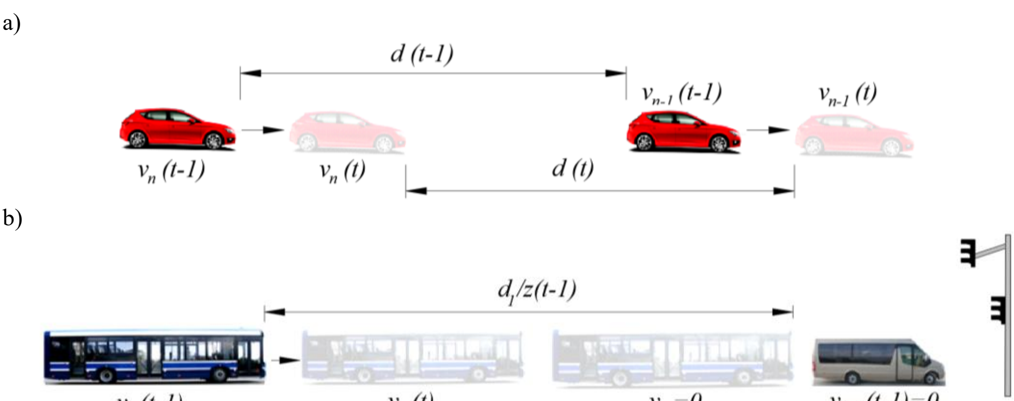

Fig. 4. Variables characterising acceleration in the fuzzy logic-based car-following model: a) vehicle immediately in front (*n* – 1) and following vehicle *n* are moving at speed *v* greater than zero, b) vehicle *n* arrives at the stopping position in the bus stop area or in the queue at the intersection entry

Test simulations were performed to determine the shapes of fuzzy sets and membership functions. During the simulation, vehicles from the data set were entered into the simulation model with information about the time of their appearance in the initial section (Fig. 3), instantaneous speed, and position in the cross section relative to the target lane, i.e., one on which the vehicle leaves the simulation area. At each simulation step, that is every $dt = 0.2$ s, the acceleration of each recorded vehicle was determined. Then it was established whether the vehicle should change lanes or be removed from the simulation area. The vehicle was removed when it passed the *SK2* intersection. Buses that reached the stopping position started passenger boarding/alighting service (the dwell time and the stopping position were entered from the database) and their speed was equal to 0 m/s until the stopped time ended. In the next steps, each vehicle was assigned a new position and lane, and vehicles that should be removed were marked. At this point, the marked vehicles were removed, and it was also verified that there was no collision of vehicles. If a collision occurred, test simulations were interrupted at that moment. In such a situation, the simulations were considered to be incorrect and the parameters and shapes of functions were changed until satisfactory results were obtained (no collisions of vehicles). Trapezoidal and triangular fuzzy sets and the normal Gaussian curve were adopted at the start of the simulations.

Multiple simulations were carried out for various combinations of dynamic parameters, looking for values that corresponded to the traffic flow in the most realistic way possible. In each simulation, the values of braking and acceleration parameters, including maximum values, were determined at the beginning in order to find out for which values the best agreement with field data could be obtained. In cases where the simulated traffic within the stop area was significantly different from real situations, e.g., in the absence of proper interaction between traffic in the lane with the stop and adjacent lanes (re-entering the traffic too fast or too late on the adjacent lane) or reaction of the vehicle to traffic lights, the situation would result in the inability of subsequent buses to enter the bus stop for passenger service. Resultant long queues of buses and other vehicles would make it impossible for buses to stop for service in the place consistent with the field data. Therefore, the location of the stopping position at the bus stop loading area, P_z, was assumed as the first criterion for testing the agreement between the simulated and real traffic flow process.

To prevent the termination of the simulation, in the absence of a place to stop in the position convergent with the field data, for model testing purposes, it was assumed that after the expiry of the adopted time interval (15 s), the passenger boarding/alighting process could start at a subsequent position (relative to the field data). The boarding/alighting process in the test simulations was assumed to take place only in the passenger service area specific for a given stop and operator (according to the measured values).

If no vehicle preceded the analysed vehicle n, a "dummy/virtual" vehicle was entered in the simulation, located at a distance of 1 km. This enabled the application of the developed algorithm also for such cases. The problem of vehicle response to traffic lights was solved in a similar manner. When the red signal was displayed, the "dummy/virtual" vehicle was placed at the stop line (speed 0 m/s). In the case of a vehicle located in a bus bay and with no vehicle in front, the "dummy/virtual" vehicle was placed at the bay exit.

Lane changes in the simulation were assumed to be consistent with field observations (field data from the databases). The vehicle's change of lane from that with the stop to the adjacent one occurred when the gap between the vehicles in the adjacent lane was long enough so that the vehicle did not have to slow down before re-entering or slowed down assuming that there could be no collision.

If the bus could not change lane due to the existing traffic situation, it braked (in accordance with the delay value determined by the function *brake rapidly*) or waited (if speed = 0 m/s) until it was possible to change lanes. In the case when the bus leaving the bay could not change lanes, it moved forward in the bay (the movement was then restricted by the vehicle ahead or by the "dummy/virtual" vehicle at the bay exit). The bus entered the bay immediately after it passed the bay entry line. Departure from the bay followed immediately after the dwell time with the value taken from the database.

The calibration of fuzzy membership functions was carried out using an exhaustive iterative search to ensure transparency and interpretability of the model results, as well as full control of vehicle dynamics in the simulation. Each simulation run was compared with field data and the optimisation criterion was

defined as the minimisation of the squared differences between the simulated and observed bus stopping positions. Data-driven or ML-based calibration approaches were not adopted due to the limited accuracy of available empirical data (e.g., lack of continuous GPS trajectories) and the need for interpretability and reproducibility of the results.
The parameter ranges tested during calibration were as follows:
– deceleration (function *brake*): 0.0–3.0 m/s²,
– acceleration (function *accelerate*): 0.0–3.0 m/s²,
– deceleration (function *brake rapidly*): 1.0–6.0 m/s²,
– acceleration (function *accelerate rapidly*): 1.0–6.0 m/s².

Incremental steps of 0.1 m/s² were applied for each variable, providing a balance between computational feasibility and calibration accuracy. Results of the analysed stopping location obtained from individual simulations were compared with the field data; squares of differences were determined and their minimum was found. Figures 5 illustrate the error surfaces obtained during the parameter search, indicating the optimal combinations of fuzzy parameters with the minimum squared difference between the simulated and observed stopping position histograms.
Figure 5 shows examples of three-dimensional maps projected onto two-dimensional surface, illustrating how to search for the best-fitting parameters of the functions describing the fuzzy sets. In this case, optimisation aimed at minimizing the squares of the difference between the histogram of the position value P_z of the buses stopped at the bus stop, generated from the simulation results, and the field data. The z axis (represented by the defined colour scheme) shows the sum of squares of differences between the frequencies in the histograms of the position P_z of the bus at the bus stop generated from the simulation results and field data. The browner the colour in the diagram, the smaller correspondence (the larger the square of difference) was observed between the simulation results and the measurement data. In cases where vehicles collided, the simulation was interrupted and the delay and acceleration values were equal to zero. In Figure 5, this area is represented by a homogeneous brown colour.
In the simulations, the impact of the slope of the analysed section within the bus stop area on the acceleration and braking ability was also taken into account. Each additional percent of upward slope reduced acceleration by -0.1 m/s² and each percent of downward slope raised acceleration by 0.1 m/s².
Analysis of the simulation results formed the basis for determining the values of vehicle movement parameters (model constants) for which the best compliance with the values observed (stopping location, lane change) was obtained. The values of the characteristic parameters of the model, established on the basis of test simulations and fuzzy logic results, were as follows:
– minimum distance between vehicles - 1.5 m,
– deceleration for the function *brake*: -1.8 m/s² for buses and trucks, -2.3 m/s² for other vehicles,
– deceleration for the function *brake rapidly*: -3.0 m/s² for buses and trucks, -5.0 m/s² for other vehicles,
– acceleration for the function *accelerate*: 2 m/s² for buses and trucks, 2.5 m/s² for other vehicles,
– acceleration for the function *accelerate rapidly*: 3.5 m/s² for buses and heavy goods vehicles, 5.5 m/s² for other vehicles,
– acceleration for the function *maintain speed*: 0 m/s²,
– maximum vehicle speed: 14 m/s.

Values of the parameters were verified again in the consecutive stage of model testing, where the lane change algorithm was extended and other model components were added. The values of dynamic parameters obtained during the simulation for individual vehicles were in most cases lower than the established limit values.

4.2. Database of adopted rules and functions

The shapes of fuzzy sets and the functions characterizing them were established on the basis of previous works in this field e.g, Ma (2006) and test simulations based on the collected field data. The fuzzy set shapes and functions define drivers' reactions to given differences in speed δv and distance d. The decision classification is fuzzy in the model. Acceleration at a given time instant is a weighted average after all decisions (with weights determined based on the shapes of the fuzzy sets) that resulted from the given logical conjunctions. The simulation model has a modular design to enable and facilitate any subsequent modifications.

a)

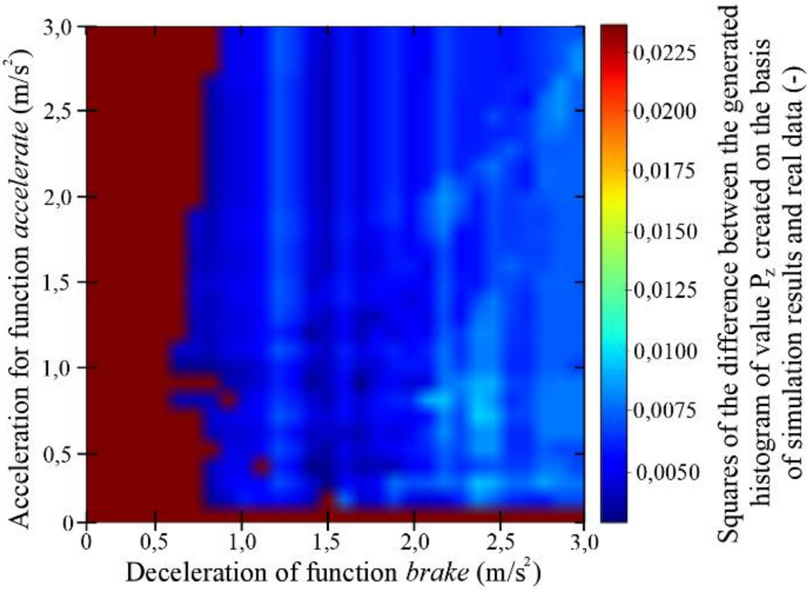

b)

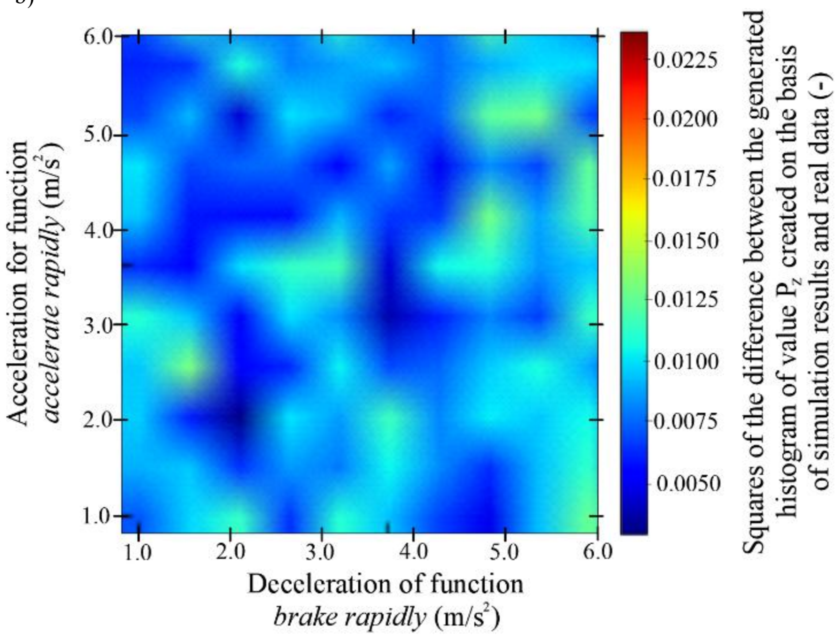

Fig. 5. Searching method for best fitting fuzzy parameters at the bus stop KIEL-03 (minimization results for P_z histograms of field and simulation data comparison) for the parameters of functions: a) *brake and accelerate*, b) *brake rapidly and accelerate rapidly*

The fuzzy sets describing the speed differences δv (m/s) were defined as follows:

– **set A1:**

$$\mu_{A_1}(\delta v)=\begin{cases}1 & \text{for } 3<\delta v\\ \frac{\delta v}{3} & \text{for } 0\le \delta v\le 3\\ 0 & \text{at the starting point}\end{cases} \quad (2)$$

– **set A2:**

$$\mu_{A_2}(\delta v)=\begin{cases}1 & \text{for } \delta v<-3\\ \frac{-\delta v}{3} & \text{for } -3\le \delta v\le 0\\ 0 & \text{at the starting point,}\end{cases} \quad (3)$$

– **set A3:**

$$\mu_{A_3}(\delta v)=e^{-\delta v^2/2} \quad (4)$$

Figure 6 shows the shapes of membership functions that describe sets A_1, A_2 and A_3.

The sets describing the distance between vehicles, d, depended on the speed of the vehicle that followed, v_n (m/s):

– **set B1:**

$$\mu_{B_1}(d)=\begin{cases}1 & \text{for } d<\xi-\sigma\\ \frac{d-\xi}{-\sigma} & \text{for } \xi-\sigma\le d\le \xi\\ 0 & \text{at the starting point,}\end{cases} \quad (5)$$

– **set B2:**

$$\mu_{B_2}(d)=\begin{cases}1 & \text{for } \xi+\sigma<d\\ \frac{d-\xi}{\sigma} & \text{for } \xi\le d\le \xi+\sigma\\ 0 & \text{at the starting point,}\end{cases} \quad (6)$$

– **set B3:**

$$\mu_{B_3}(d)=e^{-\frac{(d-\xi)^2}{2\sigma^2}} \quad (7)$$

where: $\xi=1.8v_n$, $\sigma=\xi/3$.
Figure 7 shows the shapes of membership functions that characterize sets B_1, B_2 and B_3.

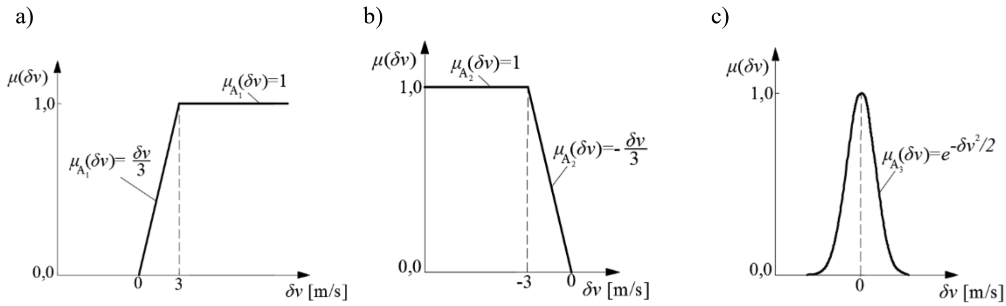

Fig. 6. Shapes of membership functions for the speed difference δv: a) set A_1, b) set A_2, c) set A_3

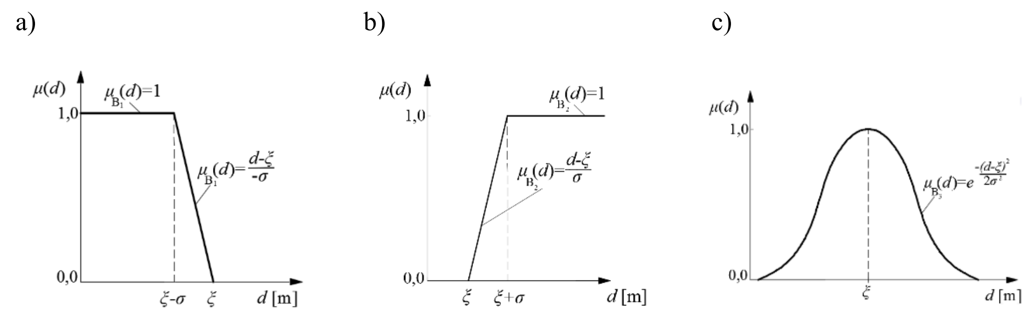

Fig. 7. Shapes of membership functions for the distance between vehicles, d: a) set B_1, b) set B_2, c) set B_3

The speed sets are two trapezoidal functions and a Gaussian function with unit variance. Based on the test simulations for the Gaussian membership function, the variance of the function was determined as the mean value (a measure of central location) divided by 3. The sets described by trapezoidal functions deviated at 3 × *variance* and -3 × *variance*. Figures 8 and 9 show examples of adopted membership functions.

4.3. Evaluation of the fuzzy logic-based car-following model for its application

Analysis of vehicle stopping position P_z formed the basis for the description of the flow of buses and other vehicles within the bus stop using the fuzzy logic-based car-following model. For this purpose, the Wilcoxon rank sum tests were performed for real and simulated observations at each analysed stop for a fixed set of parameters and adopted shapes of fuzzy sets (Table 3).

In the case of eight test sites under analysis, the hypothesis about the lack of significant differences between the distribution of real and simulated observations (at the adopted level of significance α = 0.05) must be rejected. In most cases, simulated means of position $\bar{P}_z$ were higher than those obtained from the field data. This means stopping farther from the stop exit area. A detailed analysis of the movement of individual simulated vehicles found that one of the reasons for significant differences between the field data and simulated observations may be, inter alia, lane change manoeuvres, particularly in weaving traffic zones and congested neighbouring lanes. In the simulation, this could extend the dwell time at the bus stop and thus prevent other cars from stopping at the locations consistent with those observed.

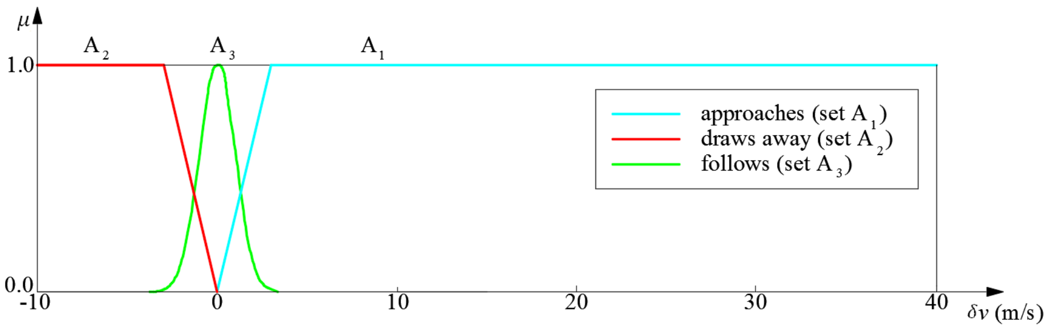

Fig. 8. Shapes of membership function for speed difference v_n

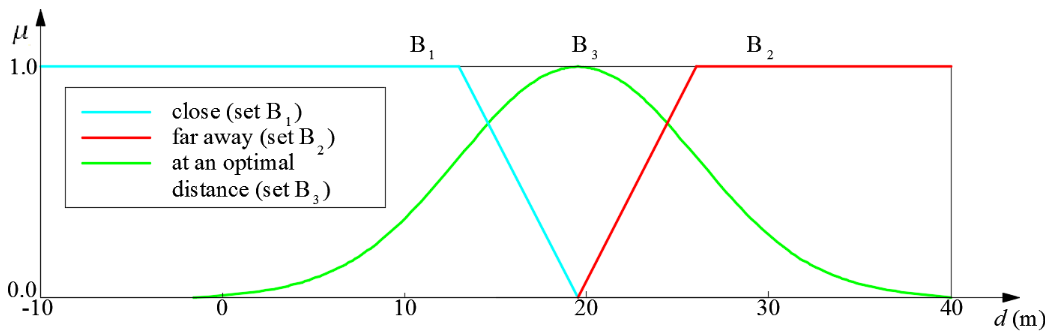

Fig. 9. Examples of membership function shapes for distances between vehicles, *d*, at vehicle speed v_n = 11.1 m/s

Table 3. Results of the Wilcoxon rank sum tests for real and simulated positions of stopping position P_z at the bus stop for buses and other vehicles, with mean $\bar{P}_z$ values

Test site (bus stop)	Average hourly traffic at the bus stop (bus/h, veh/h)			Test signifi-cance (-)	Test result	Mean value of stopping position $\bar{P}_z$ (m)	
	Urban buses	Suburban /intercity buses	Taxis and other			Mea-sured	Simu-lated
KRAK-01	40	74	40	0.01	negative	13.7	17.3
KRAK-02	52	85	32	0.16	positive	21.8	23.3
KRAK-03	39	82	66	<0.01	negative	16.0	19.3
KRAK-04	34	95	69	0.01	negative	19.2	23.4
KRAK-05	36	73	20	0.06	positive	17.8	18.5
KRAK-051	34	77	28	0.06	positive	22.2	23.6
KRAK-06	29	75	8	<0.01	negative	11.2	14.3
KRAK-07	22	93	4	0.06	positive	12.6	12.9
KRAK-08	30	90	11	<0.01	negative	10.6	11.9
KRAK-09	45	96	20	0.14	positive	19.7	19.6
KRAK-091	44	64	30	0.13	positive	15.1	15.6
KIEL-01	20	38	11	0.11	positive	16.2	17.1
KIEL-02	21	39	10	0.08	positive	17.1	18.0
KIEL-03	16	31	96	0.04	negative	22.5	25.1
KIEL-04	14	36	248	0.01	negative	5.2	6.6
KIEL-05	17	24	7	0.43	positive	21.5	22.2
KIEL-06	24	19	47	0.18	positive	10.2	10.0
KIEL-07	20	21	7	0.06	positive	5.7	5.9
KIEL-08	13	30	2	0.19	positive	13.9	14.2
KIEL-09	12	24	2	0.18	positive	8.7	9.1
KIEL-10	15	32	20	0.04	negative	21.2	24.2

The stops for which the hypothesis about the lack of significant differences between the distribution of real and simulated observations must be rejected include the test sites for which the highest number of disturbances in the movement of buses and other vehicles was recorded. As these disturbances were associated with numerous lane changes of lanes around the bus stops, the model was supplemented with the observed "courtesy" braking and delaying the movement of vehicles waiting in the queue in adjacent lanes. The algorithm that captures the above behaviour has a significant impact on the reliable mapping of driving behaviour, so it should be added at the next stage of testing the vehicle movement model. Figure 10 shows examples of histograms of stopping position P_z at the bus stop based on real-life observations and simulations for four selected test.

Despite unsatisfactory statistical test results for some of the bus stops, the differences between histograms in Figure 10 do not seem significant from a practical point of view, as these are the results of preliminary testing of the model.

5. Simulation model of the traffic flow between intersections according to the bus stop operation

5.1. General characterisation of the extended simulation model

The simulation model described in sections 4 of this paper was supplemented with additional components, including the algorithm for joining traffic and lane change. In the next stage of model testing, simulation runs were performed on a one-way road segment between intersections based on all the estimated partial models: passenger service at the stop, drivers' decisions regarding the place to stop and start passenger service, the movement of buses and other vehicles within the stop. The influence of traffic lights at the intersection before and after the stop was also considered.

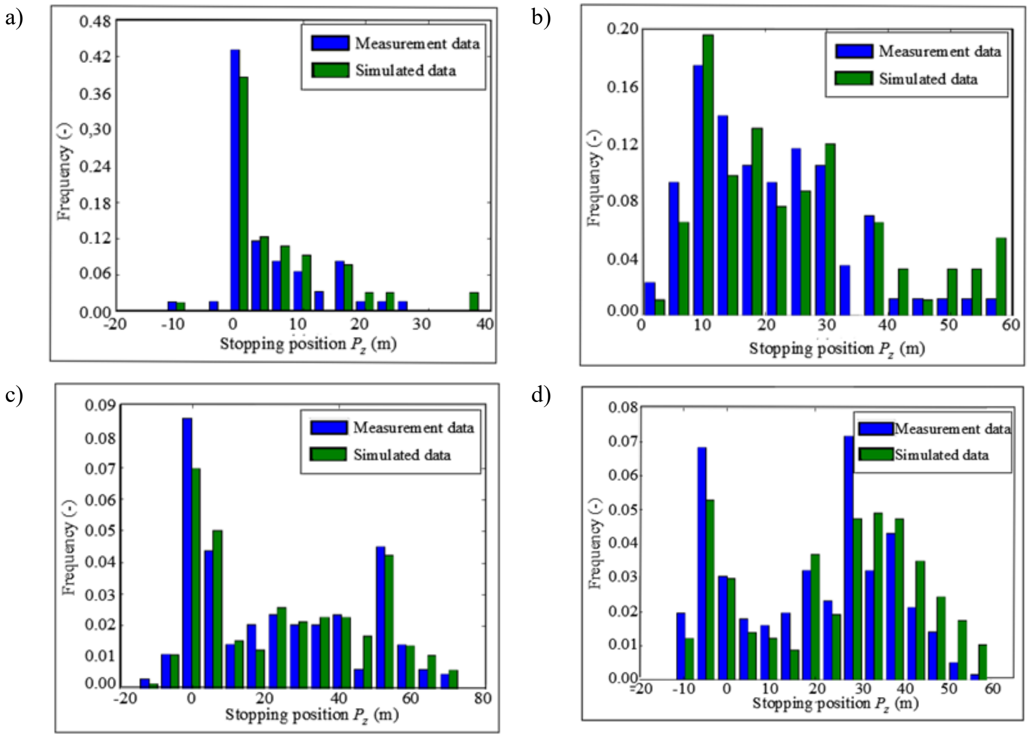

Fig. 10. Histograms of stopping position P_Z based on field observations and simulation for bus stops: a) KIEL-04, b) KIEL-10, c) KRAK-02, d) KRAK-04

The scheme of the simulation area for the segment between signalized intersections *SK1* and *SK2* for a stop located on a bus lane is shown in Figure 11. The segment covers the area between stop lines on approaches to neighbouring intersections. Analysis of that road segment was extended in relation to the analyses in sections 4 by adding an algorithm for traffic lights at the intersection before the stop. Vehicle movement from the *SK1* intersection before and in the vicinity of the bus stop is tracked and analysed. There is a right turn (1P) from entry 1, vehicles go straight ahead (2W) from entry 2, and there is a left turn (3L) from entry 3, as shown in Figure 11. The distribution of individual vehicles for each manoeuvre into particular lanes is made for the segment in the vicinity of the bus stop. The assumed cross-sections in which vehicles appear in the simulation area are located at entries 1, 2 and 3 of the *SK1* intersection.

Separate steps of the simulation program were graphically represented by flowcharts describing the appearance of vehicles in the simulation area, their movement, passenger service at the stop, lane changes and vehicles leaving the simulation area. Figure 12 shows a general flowchart of the simulation that was translated into Python programming language. In the program structure, individual vehicles are objects to which specific input data are assigned (vehicle length, bus operator type, information about the necessary lane change, and others). The general layout of the simulation program consists of 4 blocks, where block B1 is the part related to entering the input data characterizing the analysed segment and individual vehicles in the simulation. In this block, the so-called waiting table with all vehicles sorted according to their time of appearance in the generation cross-section.

Separate vehicle lists are created for each of the lanes. For each lane of a given link, vehicles (objects) were entered into the presence table in the subsequent time steps with the assigned characterisation parameters. The clock regulating the movement of vehicles changes by *dt* at each simulation step. In block B2, vehicles are introduced in an appropriate sequence to the analysed segment through the so-called presence board. The simulation ends when the wait board and the presence board are empty. When the current simulation time is equal to the current time of crossing the initial cross-section, the next vehicle is entered into the presence board (on the appropriate lane), and the numbering in the waiting list is decreased by one $(np = np - 1)$. If this is not the case, the time *ts* is increased by *dt* and a check is made again whether the waiting and presence lists are empty.

The traffic situation analysis block (B3) takes into account all partial models developed to map the traffic flow on the segment between intersections, including: selection of a stopping position at a bus stop, passenger service, vehicle movement, lane changes and traffic light operation. Due to its extensive form, block B3 will be discussed separately.

In block B4, simulation results are collected and parameters characterizing the traffic flow on the analysed segment are calculated, including the measures for assessing traffic conditions, service quality at the stop, such as:

– delays d_{z1} (s/veh), (s/passenger) incurred by buses in the queue before the stop,
– probability P_{dz1} (%) of queueing before the stop due to stopping position obstruction by preceding buses,
– average and maximum length of the queue of vehicles before the stop,
– delays d_{z2} (s/veh), (s/passenger) incurred by buses due to the inability to depart from the loading area,
– probability P_{dz2} (%) of delays resulting from the inability to depart from the stop after ending passenger exchange, delays on the part of other vehicles moving in the vicinity of the stop, including the delays due to disturbances in the vicinity of the stop (additional time needed for covering the distance within the stop - in relation to the travel time without disturbances) resulting from the delay or delay and stoppage.

The calculated delays may be referred to the bus (s/bus), other vehicles (s/veh) or a passenger (s/passenger).

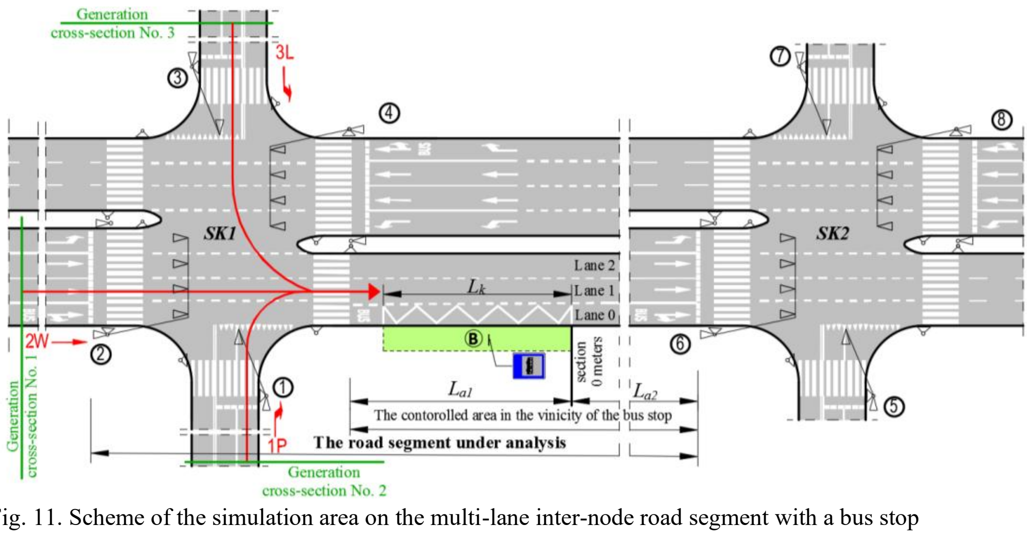

Fig. 11. Scheme of the simulation area on the multi-lane inter-node road segment with a bus stop

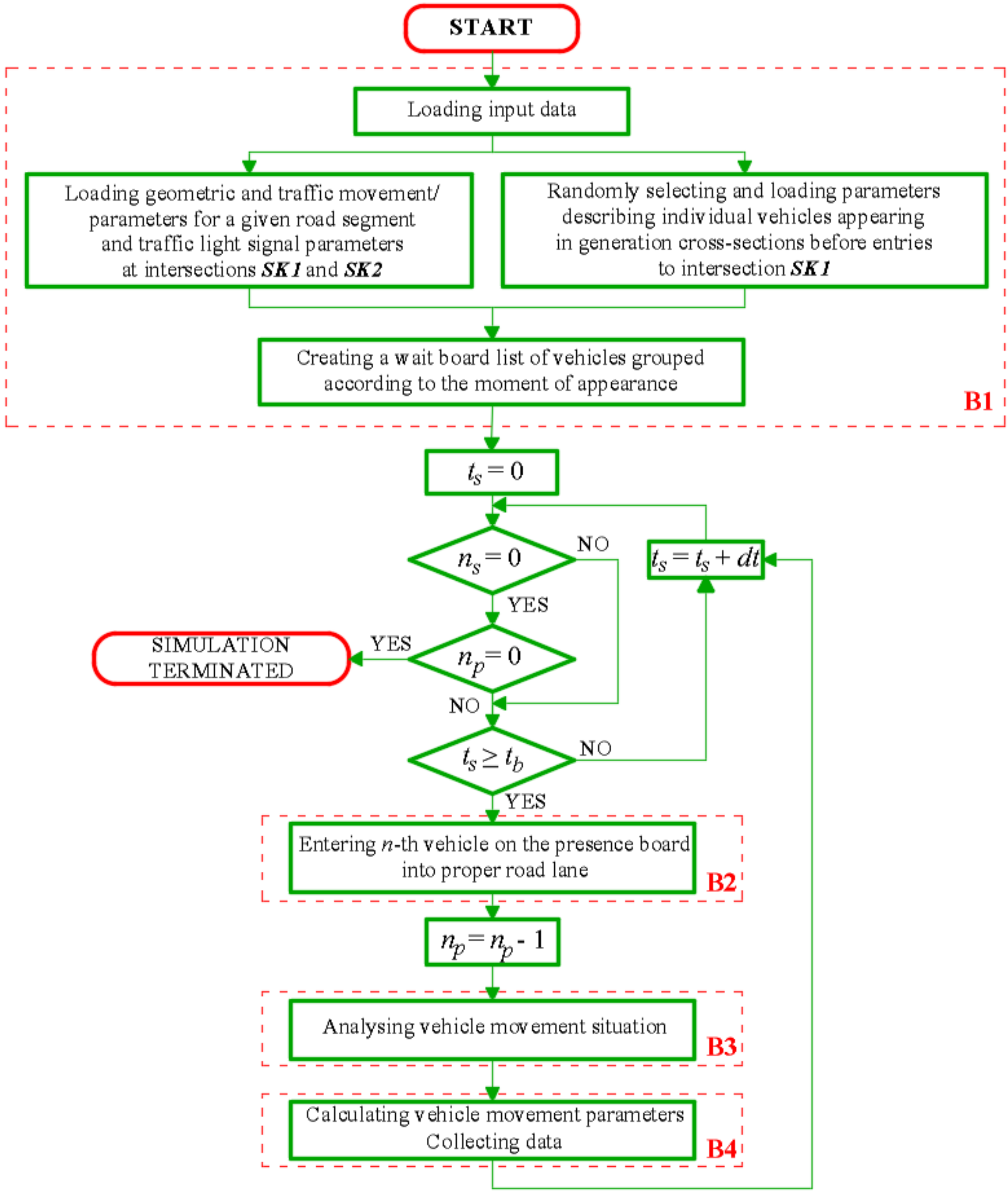

Fig. 12. General flowchart: t_s – current time of simulation step, dt – number of vehicles in the waiting table, t_b – current time of crossing the initial cross-section by the n -th vehicle

5.2. Random parameters from vehicle generation in the simulation model

Random parameter generation reflects the stochastic nature of real-world traffic at urban bus stops, where arrival times, vehicle types, and duration of passenger service vary unpredictably. Using random distributions ensures that simulation outputs represent a realistic ensemble of possible traffic states, allowing statistical evaluation of system performance rather than deterministic single-case outcomes.

The around-bus-stop traffic simulation program generates random values of parameters describing individual vehicles appearing in generation cross-sections in terms of arrival times, vehicle characteristics or passenger service. The randomly selected parameters are listed in Table 4. The program can generate multiple streams of different vehicle groups.

Random generation of model parameters was based on standard probability distributions commonly applied in microscopic traffic and transit simulation. In the vehicle movement module, the desired speed and desired stopping position were generated from normal distributions, reflecting the variability of driver behaviour observed in empirical studies (e.g. Treiber and Kesting 2013). The time intervals between vehicles appearing in the generation cross-sections followed an exponential distribution, corresponding to a Poisson arrival process independent for each vehicle stream (e.g. Leungbootnak et al. 2025). The type of vehicle, entry, and lane number were drawn from a discrete multinomial distribution, adopted based on sources from the literature and the generally recognised stochastic characteristics of these variables. In the passenger service module, the spatial distribution of waiting passengers followed a beta distribution, the numbers of boarding and alighting passengers a Pascal (negative binomial) distribution, the individual boarding and alighting times a lognormal distribution, the passenger walking speeds a normal distribution and the post-service technical time a gamma distribution. These latter distributions were determined from field observations and empirical data.

The parameters of all distributions were estimated using Maximum Likelihood Estimation (MLE) and Maximum Goodness of Fit (MGF–AD) methods with the Anderson–Darling statistic as an estimator. The detailed formulation and validation of these estimation procedures are presented in the previous work (Stępień 2017). This approach ensured that the stochastic nature of vehicle–passenger interactions observed in the field was accurately reflected in the simulation.

The time interval between the vehicles appearing in the generation cross-sections at the *SK1* intersection entries follows exponential distribution (Poisson process independent for each stream of vehicles with the constant λ parameter) based on the given vehicle traffic volume *Q* (veh/h).

Vehicles appear outside the controlled area, in front of the signalized intersection (cross-section no. I, II, III), if it is located before the stop. If there is no place for a vehicle to appear at the randomly selected point in a given cross-section, then the vehicle is queued and waits until the place of appearance becomes free.

The data collected during the study was the basis for generating four independent streams of vehicles grouped (*Gr_poj*) as urban buses (Q_{Am}), coaches (Q_{Az}) taxis and other vehicles (delivery vans, passenger cars, emergency vehicles) Q_{tds} running along the lane with a bus stop or entering the bus stop bay, and vehicles in the neighbouring lanes (Q_{ps}). Percentage contribution of each vehicle type is established within each vehicle group. For urban buses, the percentage of large-capacity, medium-capacity and low-capacity vehicles was established. For coaches, the program can classify vehicles according to, for example, vehicle length.

The generated bus/vehicle is assigned to one of the intersection entries (*ID_wl*) based on the given traffic direction structure. This is done in such a way that first all λ parameters given for each entry and for each vehicle type are added up. On the basis of this sum, the moment of the vehicle appearance is calculated from the exponential distribution. The group of vehicles (*Gr_veh*) and the intersection entry number (*ID_wl*) are generated from the multipoint distribution with probabilities calculated by treating the λ parameters as weights.

Table 4. Parameters of buses, other vehicles and passengers, and the character of random variables selected in the input data blocks.

Parameter	Description	Generation of parameter random values	Set parameters
$\Delta\boldsymbol{T}$ (s)	Time interval between vehicles appearing in generation cross-sections	Exponential distribution (Poisson process independent for each vehicle stream)	Vehicle traffic/bus traffic Q (veh/h)
$\boldsymbol{Gr\_veh}$ (-)	Vehicle group (bus operator type)	Multi-point distribution	Traffic type structure –percentage contribution of vehicles of given groups at entries of intersection *SK1* u_{wl} (%) and traffic lanes u_i (%)
$\boldsymbol{T\_veh}$ (-)	Vehicle type by length and number of doors for passengers	Multi-point distribution	Traffic type structure –percentage contribution of vehicles of given type u_{Tp} (%)
$\boldsymbol{ID\_wl}$ (-)	Intersection entry number, where a vehicle appears	Multi-point distribution	Traffic direction structure - percentage contribution of vehicles/buses at entries of the intersection u_{wl} (%)
$\boldsymbol{ID\_lane\_i}$ (-)	ID number of the lane, where a vehicle appears at the moment it enters the analysed area	Multi-point distribution	Traffic direction structure - percentage contribution of vehicles from a given entry on lanes u_i (%)
$\boldsymbol{ID\_lane\_j}$ (-)	ID number of the lane, where a vehicle leaves the analysed area	Multi-point distribution	Probability of lane change independently for each traffic lane u_{zp} (%)
$\boldsymbol{n_{ws}}$ (passenger/bus)	The number of passengers boarding	Negative binomial distribution	Mean value $\bar{n}_{ws}$ and standard deviation $\sigma_{n_{ws}}$ of the number of passengers boarding (passenger/h)
$\boldsymbol{n_{wys}}$ (passenger/bus)	The number of passengers alighting	Negative binomial distribution	Mean value $\bar{n}_{wys}$ and standard deviation $\sigma_{n_{wys}}$ of the number of passengers alighting (passenger/h)
$\boldsymbol{x_p}$ (m)	Location of the waiting position for passengers at the bus stop	Beta distribution	Mean value $\bar{x}_p$ (m) and standard deviation σ_{x_p} (m) of the waiting area for passengers, the beginning $x_{p,0}$ (m) and end $x_{p,1}$ (m) of the waiting area

After passing the *SK1* intersection, the vehicle of the specified route enters the controlled area and occupies one of the lanes in the vicinity of the bus stop. The lane ID number (*ID_lane_i*) is generated from the multi-point distribution, but the probabilities of selecting individual lanes are calculated differently than for the vehicle type and intersection entry number. The user gives two sets of weights. The first set is for a specific entry and the second is for a specific vehicle type. The product of the weights is the basis for calculating the probability of multi-point distribution.

Some of the vehicles change lanes within the analysed area. The model allows each vehicle to change the lane. The probability of changing the lane from lane i to lane $j(u_{zp})$ is given in the form of a matrix, separately for each type of vehicle.

The type of vehicle (*T_veh*) determines its length, capacity and the number of doors. For each type of vehicle, the user provides a list of vehicle types that may appear, along with the percentage contribution in the traffic. On this basis, the vehicle type is generated from the multi-point distribution.

Passenger numbers are modelled using the Pascal distribution (negative binomial distribution). It is a discrete distribution, unlimited on the right side, defined by two parameters p and r. Both parameters of the distribution are given separately for each group of vehicles and separately for boarding and alighting passengers.

Values of parameters α and β of the beta distribution are also given at the start. From this distribution the positions of passengers waiting at the x_p stop are generated based on the measured or predicted average value $\bar{x}_p$, standard deviation σ_{xp}, and the range of the waiting area at the bus stop (ends of variability ranges $x_{p,0};x_{p,1}$). These parameters are established for two separate groups of users, i.e., passengers of the urban bus operator and *other users*.

5.3. Characteristics of the method of mapping vehicle movement in the area of analysis

The traffic situation of the vehicle moving along the test segment is affected by the driver's reaction to the current traffic conditions, which in turn determines the value of acceleration and deceleration and the vehicle stops, as described in sections 4. The road traffic efficiency in the analysed segments is also influenced by traffic lights parameters at adjacent intersections, passenger service at the stop, the manoeuvres of vehicles changing lanes and buses re-entering the traffic stream. Flowcharts in figures B.1, B.2 and B.3 (Appendix B) illustrate the traffic situation of buses and other types of vehicles moving in the simulation area. These diagrams are an extension of block B3 shown in Figure 12. Block B3.2 is a simulation block of the passenger service process used to calculate the passenger service time.

For each subsequent time step of the simulation, the vehicle acceleration (deceleration) value is determined depending on the traffic situation and the speed of the analysed vehicle. It results from the conditions of dependent driving described by fuzzy logic rules in accordance with the developed vehicle movement model for the road segment in the vicinity of the bus stop (sections 3). The analysis also covers the traffic lights operation and the need to change lanes and stop at the bus stop. When the current phase of the traffic lights or the traffic conditions at the stop do not allow the movement with the calculated acceleration (or deceleration), these dynamic values are corrected. Phases of traffic light operation influence the formation and discharging of vehicle queues (block B 3.1). When the vehicle passes the *SK2* intersection, it leaves the simulation area.

Before starting the simulation in block B1, the values of the analysed segment geometric and movement/traffic parameters and the parameters of traffic lights at intersections *SK1* and *SK2* are loaded. These are the following:

– the distance from the *SK1* intersection (before the stop) to the stop's front (assumed cross-section of 0 meters) L_{a1} (m),
– the distance from the front of the stop (section 0 meters) to the conditional stop line at intersection *SK2* (behind the stop) L_{a2} (m),
– the number of lanes in the road cross-section within which the stop is located,
– parameters of the implemented traffic lights program upstream and downstream of the bus stop,
– longitudinal inclination of the road where the bus stop is located i (%),
– the average location of passengers waiting at the stop for the urban bus operator $\bar{x}_{p\_m}$ (m) and for other users $\bar{x}_{p\_pu}$ (m),
– standard deviation of the location of the passenger waiting area at the stop for the urban bus operator σ_{xp_m} (m) and for other users σ_{xp_pu} (m),
– ends of the variability range for the location of the waiting position at the stop for urban bus operator passengers $[x_{p,0\_m}; x_{p,1\_m}]$ (m) and *other users* $[x_{p,0\_pu}; x_{p,1\_pu}]$ (m),
– location of the beginning and the end of the *passenger boarding/alighting area* $[x_{wp,0}; x_{wp,1}]$ (m).
– Each vehicle appearing in the simulation procedure is described by the values of block B1 parameters generated from adequate algorithms:
– the ID number of vehicle n that identifies this vehicle and allows simulation result analysis,
– vehicle type (model, length),
– operator bus type (urban, suburban, intercity, taxis and other vehicles, vehicles in the lanes adjacent to the bus stop),
– the ID number of *SK1* intersection entry, at which a vehicle appears in the generation cross-section,
– manoeuvre type at the *SK1* intersection (1P, 2W, 3L),
– the ID number of the lane with the vehicle at the entry to the controlled area i (-),
– the ID number of the lane with the vehicle at the exit from the controlled area j (-),
– the number of passengers boarding the bus n_{ws} (passenger/bus),
– the number of alighting passengers n_{wys} (passenger/bus).

After entering the controlled area, vehicles are assumed to seek lane change in the desired direction of the intended manoeuvre at the intersection. Thus, the position of the vehicle in relation to the desired lane is determined (the lane on which the vehicle is when leaving the simulation area) and the possibility of making the lane change manoeuvre dependent on the traffic conditions and vehicle speed is analysed. The manoeuvre is made if the conditions in neighbouring lanes allow the change according to the developed algorithm.

After a vehicle appears in the controlled area in the bust stop zone, its movement situation depends on the necessity to stop at the bus stop and traffic lights at intersection *SK2*. If the vehicle handles passengers at the bus stop $(n_{ws+}n_{wys}) > 0$ on a traffic lane other than the lane on which the bus stop is located (or the bus stop is in a bus bay), the lane change manoeuvre is made. The vehicle at the bus stop serves passengers at the location generated according to the stopping position selection model, described in a separate paper (Stępień 2017). Due to different stopping position chosen by different bus operators, an algorithm for making decision about starting the bus passenger service was added. The vehicle at the bus stop starts the passenger service or waits in queue for the opportunity to approach the passenger boarding/alighting area. The time spent at the bus stop is a sum of dwell time, clearance time, and delays incurred by queueing and re-entering the traffic stream.

The flowcharts in figures 12 and B.1 (Appendix B) represent a situation when a single lane change is performed in the vicinity of a bus stop. When more than two lanes are present, additional lane changes can be performed to reach the desired lane at intersection *SK2* (forced lane change).

5.4. Algorithm of the traffic lane change mode and re-entering the traffic stream onto the adjacent lane after passenger service

Due to the model's insufficient accuracy in the description of lane change manoeuvres, appropriate algorithms were extended to cover the cases with queues present on adjacent lanes at all times (as at the bus stops KRAK-01 or KIEL-03). In the simulation with the first tested version of the program, compared to the real-world observations, the waiting time at the stop was substantially longer due to the inability of the bus to re-enter the traffic stream in the adjacent lane. The extended simulation model made distinction between two lane change modes: a forced lane change (mandatory) and a free lane change (discretionary). A possibility of passing the preceding vehicle was added to the model under the following assumptions:

– the vehicle completed passenger service and other necessary activities ended (clearance time),
– the vehicle's current speed is $v_n = 0$ m/s,
– the vehicle is in lane *j* where it exits the simulation (otherwise a forced lane change will be performed),
– the current speed of the vehicle in front is $v_{n-1} = 0$ m/s.

Moreover, for the case of the free lane change, it was assumed, based on the video data analysis, that the probability of passing (randomized once per passing attempt) is 0.02 for urban buses, 0.7 for suburban and intercity buses and 0.95 for other buses and vehicles stopping at the bus stop.

Analysis of vehicle turning parameters was the basis for the assumption that the minimum distance between the vehicles necessary to perform the passing manoeuvre was 4.0 m for urban and intercity buses, and 2.0 m for other buses and vehicles. The described situation also applies to lane changes made to the adjacent lane downstream of the bus stop by vehicles that did not provide passenger service at the stop.

In order to change lanes, the driver has to find an appropriate time gap in the traffic flow on the adjacent lane, which is a function of the lane-changing vehicle's speed as well as the speed and position of vehicles in the adjacent lane. It results from dependent driving (following) conditions described with fuzzy logic principles in accordance with the developed model of vehicle movement on the street section in the vicinity of the bus stop.

The model also includes the so-called "courtesy" yielding or a delay in moving forward in the queue to enable a bus to change lanes from the adjacent bus lane. Based on the video material collected, it was assumed in the model that the speed of the vehicle that gives way is relatively low and amounts to $v_{ps} \leq 7$ m/s. In the simulations, the "courtesy" merge takes place with the assumed probability of 0.5 in each subsequent step of the simulation, and this probability increases with time. This algorithm considerably improves the reliability of the representation of drivers' behaviour when re-entering the traffic stream from the stop. The lane change manoeuvre of the vehicle *n*, including the "courtesy" yielding, is shown in Figure 13.

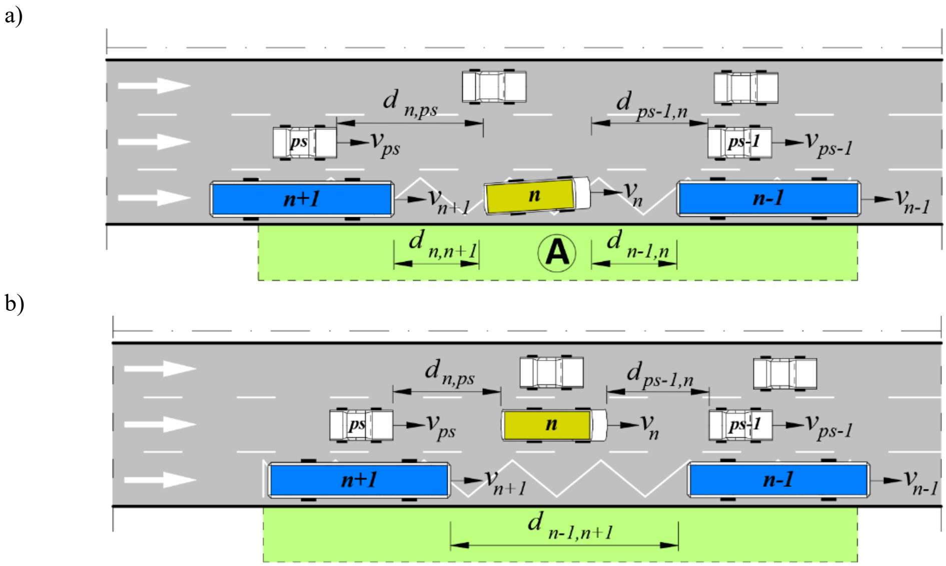

Fig. 13. Illustration of the lane change manoeuvre with "courtesy" yielding: a) the moment at which the driver of the vehicle n decides to change lanes, b) the next moment - after the vehicle n performs the lane change manoeuvre, where: n - the vehicle performing the lane change manoeuvre, ps - vehicle in the adjacent lane, in front of which the vehicle n enters the traffic, v - vehicle speed, d - distance between vehicles

In the first phase of the lane change manoeuvre, the movement of vehicle n depends on the preceding vehicle $n-1$ and parameters v_n, d. The movement of vehicles ps and $ps-1$is observed to see whether a lane change is possible. After making the decision to change lanes, the movement of vehicle n starts to depend on vehicle $ps-1$.

After the simulation test runs (vehicle movement around the bus stop, lane change manoeuvres), an additional parameter was adopted, i.e., the driver's reaction time $t_r = 0.6$ s. This value is consistent with the current state of research in this field (Krystek 1980) and was determined based on the comparison between the simulated manoeuvres and the video data recorded.

For each successive time step of the simulation, the vehicle acceleration (deceleration) value $a_n(t+t_r)$ is determined depending on the current speed of the vehicle v_n, the speed difference between the vehicles δv and the distance d between the vehicles. It results from the dependent driving conditions (following) described using the resulting fuzzy logic principles. The value $a_n(t+t_r)$ is calculated for each vehicle as a weighted average with weights in the interval [0,1] resulting from membership functions $\mu(\delta v)$ and $\mu(d)$, which determine the type of events. The resulting functions (*brake, brake rapidly, maintain speed, accelerate, accelerate rapidly*) determine the limit value of acceleration (deceleration) with values depending on the type of vehicle (buses and trucks, other vehicles) and the values of the average longitudinal inclination i (%) of the road segment where vehicle queues form.

In the absence of traffic restrictions related to the movement of preceding vehicles, the conditions in the adjacent lane or the operation of traffic lights at intersections, the vehicle accelerates to the desired speed V_{np}, which follows a normal distribution with parameters $\bar{V}_{np}$= 14 m/s and $\sigma_{v_{np}}$=1.4 m/s.

5.5. Algorithm of making decision about stopping and starting passenger service at the bus stop

Analysis of the collected video material and measurement data showed a need to develop an additional algorithm to represent the randomness of decisions made by drivers to start passenger service. Different groups of bus operators stop to serve passengers at different bus stop areas. Urban buses typically occupy the berths that are closest to the exit of the stop area and in close proximity to the vehicle in front. Observed cases of choosing a stopping position at greater distances indicated the need to include such situations in the model. *Other users* stop to serve passenger movement near the entry of the stop at a large distance from its exit (several or several dozen meters) even when there are no other vehicles at the stop. Within each stop, it is possible to distinguish characteristic passenger service areas and areas which drivers never use for this purpose. It is also possible to distinguish a certain section of the stop, where some drivers serve passengers, and some wait to occupy the position closer to the exit when there are two or more buses in front of them. Such an area is defined as a *dilemma zone*. To reflect the randomness of drivers' behaviour in this zone, it was established that the decision to start passenger service would be influenced by passenger distribution at the stop, the arrival time of the first boarder t_{dpas} and the time gap between the stopping of the analysed vehicle and the departure of the preceding vehicle t_{dodj} (Fig. B.2 – Appendix B). It is less important in the case of urban buses, but it is clearly noticeable for *other users*, where a passenger, when approaching the vehicle, initiates service at a given location.

The stopping position at the stop is selected in accordance with the model described in a separate paper (Stępień 2017) . In that model, the area P_z is estimated separately for the urban operator and for *other users* (suburban and intercity buses, private cars, taxis and other vehicles). Due to the large influence of the random factor, this position is generated from the normal distribution with the mean calculated from multiple regression models and determined standard deviation. The distribution is cut on both sides because *the loading area* is established individually for a given stop with a defined maximum range resulting from the location and the specificity of bus stop operation. The *loading area* may be larger than that defined by geometric parameters (length of the boarding/alighting line in a bay) or traffic organization (line of road markings) and limited by the location of pedestrian crossings, intersection entries, etc. In addition to the type of bus operator, the multiple regression model takes into account the traffic conditions, boarding passenger service or lack thereof, and the number of vehicles approaching behind the analysed vehicle.

In the simulation model, passenger service starts each time the bus stops at the position defined by the geometric parameters of the stop or traffic organization (length of the boarding and alighting area limits). Cases of boarding and alighting outside the designated zone (third and subsequent positions) and the random nature of decisions about passenger service commencement made by the bus driver led to the introduction of the concept of a *representative waiting area* for passengers, calculated individually for each stopped vehicle. It is a section of a bus stop that defines the range of the bus positions for which no delays related to the arrival of the first passenger are incurred with the time for passenger alighting operation taken into account. The time of first passenger getting on the bus stopped at P_z is calculated on the basis of the randomly generated location of the waiting passenger x_p and speed V_{pas} (normal distribution with parameters $\bar{V}_{pas}$ = 1.93 m/s and $\sigma_{v_{np}}$= 0.3 m/s).

In the case where none of the passengers alight, the *representative waiting area* is within the minimum to the maximum waiting location, x_p. These boundaries are extended to the farthest distance the passenger can walk to board the bus, moving from the waiting location x_p at a random speed V_{pas} at time t_{odj} counted from the moment the bus stops until the departure of the vehicle occupying the berth closer to the exit. It was also assumed that the *representative waiting area* for a bus cannot be greater than the designated *loading area* at the stop. In addition, the decision by the vehicle driver to start passenger service outside the designated boarding and alighting limits has a probability of 0.3 for the urban bus operator and 0.8 for *other users.*

As for alighting passengers, the alighting time is calculated as the sum of the individual alighting times for each passenger in accordance with the passenger service time model described in separate paper (Stępień 2017). The boundaries of the *representative waiting area* are then extended to the farthest points a passenger can walk to board the bus, moving from the waiting location x_p during *the alighting time* at a random speed $V_{pas.}$

In a situation when the time t_{odj}, counted from the moment the bus stops in a queue and waits for the leading bus to depart, is shorter than the calculated first passenger walk time t_{dpas}
the passenger service does not start and the vehicle moves to the place closer to the exit, in accordance

with vehicle movement model. Otherwise, the model starts passenger service simulation also when the vehicle is stopped outside the designated loading area.

6. Model verification and validation

In order to verify the overall simulation model, test simulations of traffic flow were carried out on all partial models. A total of 100 simulation runs were performed for all analysed stops and covered the area within which the impact of bus stops on traffic efficiency in the adjacent lanes was observed.

The traffic situation at the stop (vehicles stopping for passenger service and waiting in the queue) affects the way other vehicles move in its vicinity at a given time (acceleration a_n, speed V_n, position P_n), contributes to delays and queues, and affects lane change and merging manoeuvres.

The result evaluation method used at this stage differed from that adopted in section 5 of this study. Individual results of the actual measurements (for each bus) were compared with the distribution of individual parameter values from 100 completed simulation runs.

In order to verify the traffic flow model and lane change algorithm, the following the following variables were analysed:

- T_{p_z} – the time from the moment the vehicle appears in the controlled area until it stops in the loading area for passenger service,
- T_{kw_zn} – the time from the passenger service completion until disappearance from the controlled area,
- T_{p_zn} – the time from the moment the vehicle appears in the controlled area until it disappears from that area.

For each simulated vehicle, the statistics of the parameters above were calculated for the data obtained from 100 simulations. These were the mean, standard deviation, median, minimum value, maximum value and auxiliary measures, called in this study *PROC*, *SDDIST_PROC* used for the interpretation of the simulation results. The *PROC* values were adopted as the basic measure for the analysis of the simulation results.

The calculated measures (*PROC*) indicate the percentage (percentile) of the measurement result against the simulated values. Variables with a *PROC* prefix determine the value of the cumulative distribution function for the recorded measurement value, that is, the contribution of the number of simulations, whose result is lower or equal to the given value recorded during the measurements.

The values of the calculated *PROC* variables range from 0 to 1. The distribution of the calculated *PROC* measures is the basis for assessing the agreement of the simulation results with the measured values. The null hypothesis is that the measured value has the same distribution as that calculated for the simulation values. If the simulation results are in perfect agreement with the measurement results, then a uniform distribution of variables with the *PROC* prefix should be expected.

The measure called *SDDIST* is the difference between the mean value obtained from the simulation and that from the measurements, calculated in units (multiciplity) of standard deviations of the simulated variable distribution. It is a *z-score* statistic or a standard score. Statistical significance calculated for this variable should be approximately equal to the significance calculated based on the variable with the *PROC* prefix. It corresponds to a parametric test for the agreement of the empirical value with the mean from the simulation. The statistical measure *SDDIST_PROC* which is the probability value of a one-tailed statistical test was used in the analysis. In order to calculate this measure, the so-called Gaussian error function (*erf* (*SDDIST*)) was used.

The model was also verified using the data measured at the bus stop "Warszawska/Politechnika" (KIEL-11) in Kielce. These data were not used for building the simulation model.

In order to assess the agreement of the simulation results with the measured values, the distributions of the calculated *PROC* and *SDDIST_PROC* measures for selected variables were presented. Three groups of vehicles were analysed: buses of the urban bus operator (*m*), buses and other vehicles of *other users* group at the stop (*pu*) and the vehicles in the lanes adjacent to the stop (*ps*).

Analysis of the *PROC* measure for variable T_{p_z} allows verifying whether the bus run times from appearing to stopping at the berth, queues, and delays are correctly represented. Figure 14 shows *PROC*_T_{p_z} histograms.

The percentage of vehicles in the ranges shown in Figure 14 is from approx. 9.8 % to approx. 10.3 %. Analysis of *PROC* distributions for variable T_{p_z} shows that most values of the calculated measures are in the range 0.4 to 0.5. Approximately 1.9 % of the simulation results show non-compliance with the T_{p_z} measurement data for urban buses, and approx. 0.9 % for *other users*. These values were estimated as the sum of PROC value percentage above and below the level of 10 % (dashed line in the graphs) against a uniform distribution of the calculated measures.

Figure 15 shows the distribution of *PROC* values for the time from the completion of passenger service to the moment when the vehicle disappears from the simulation area T_{kw_zn}. Analysis of this measure allows, with the use of the developed lane change algorithm, evaluating the course of the simulation process from the completion of passenger service to the moment of re-entering the traffic stream.

In the case of variable T_{kw_zn}, the percentage of the *PROC* measure contribution ranges from approx. 9.7 % to approx. 10.4 % for urban bus operators and from approx. 9.6 % to 10.5 % for *other users*. The values of *PROC* measures are most often in the range 0 to 0.1 and 0.9 to 1.0 for urban bus operators, and from 0.5 to 0.6 and 0.9 to 1.0 for *other users*. Approximately 1.9 % of simulation results for urban operators and 2.3 % for *other users* did not agree with the measurement data estimated relative to the 10% level.

Analysis of the *PROC* measure for the T_{p_zn} variable shows whether the travel time from the appearance to the disappearance of the vehicle from the observed area is properly represented. Figure 16 shows the histograms of the measures *PROC*_T_{kw_zn}. Figure 17 shows the histograms of the *SDDIST_PROC*_T_{p_zn} values. Histograms of the calculated measures are presented separately for urban bus operators (Fig. 16, 17 a), *other users* (Fig. 16b, 17b) and vehicles moving in the lanes adjacent to the stop (Fig. 16c, 17c).

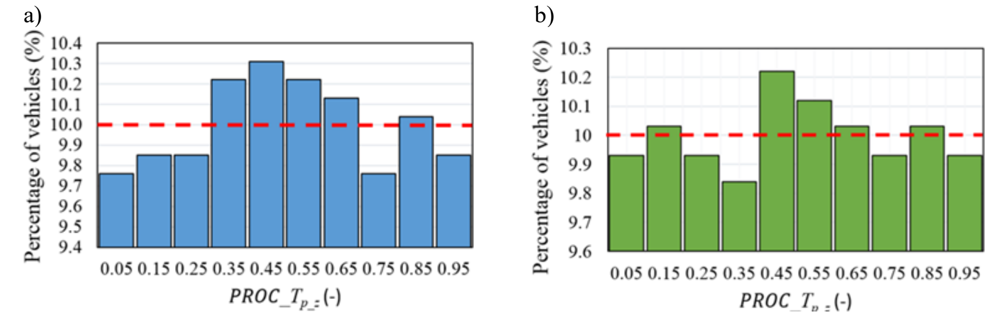

Fig. 14. Histograms of *PROC*_T_{p_z} values for the time period beginning at the appearance of the vehicle in the controlled area and ending at the moment the vehicle stops for passenger service: a) urban buses, b) *other users*

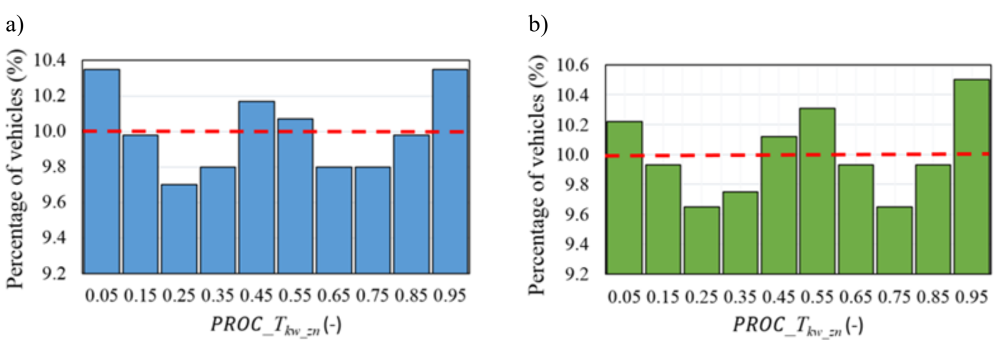

Fig. 15. Histograms of *PROC*_T_{kw_zn} values for the time period between the end of passenger service and disappearance from the controlled area: a) urban buses, b) *other users*

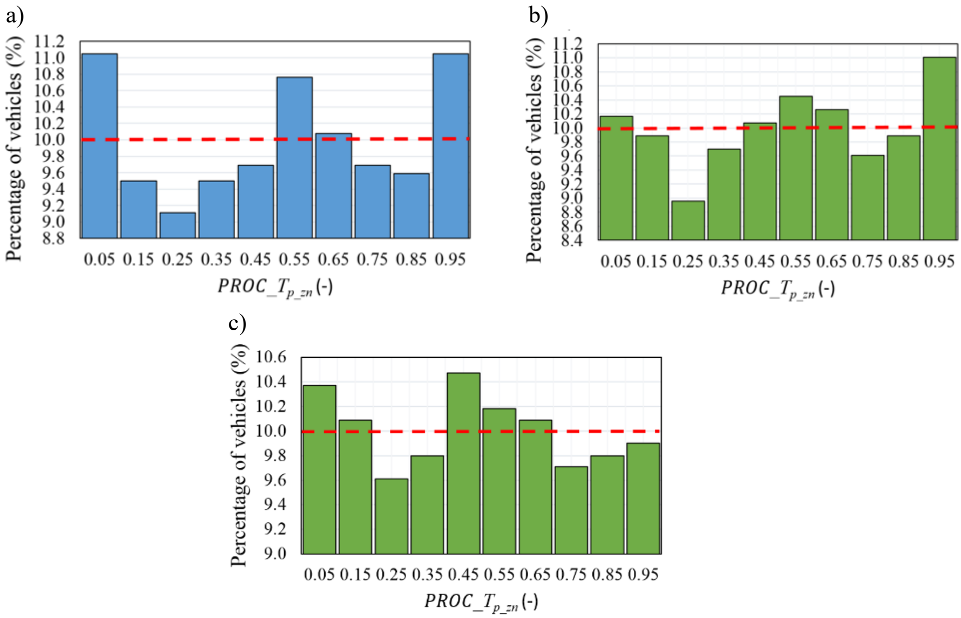

Fig. 16. Histograms of $PROC\_T_{p\_zn}$ values for the time period between the appearance of the vehicle in the controlled area and the disappearance from that area: a) urban buses, b) other users, c) vehicles in adjacent traffic lanes

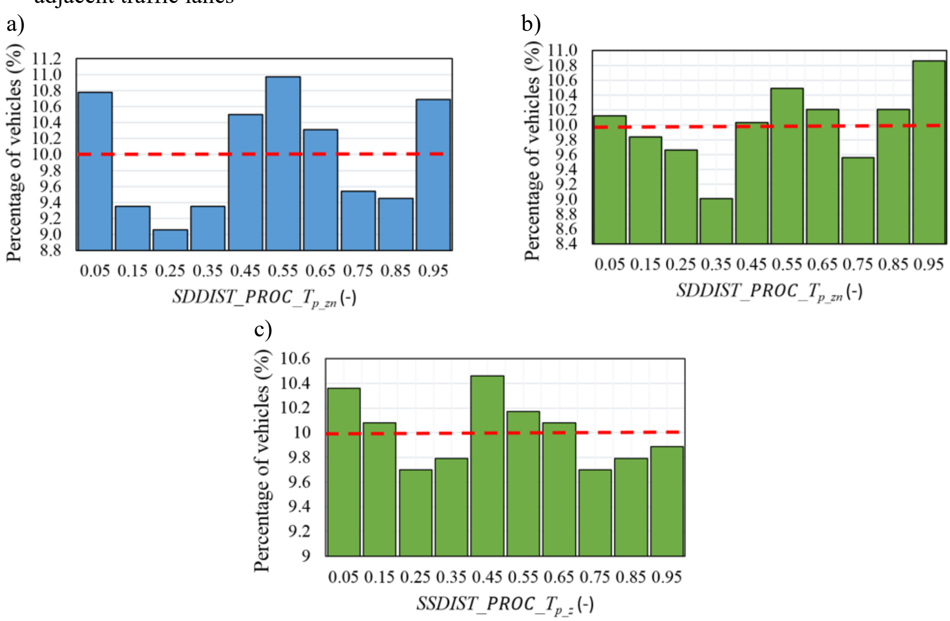

Fig. 17. Histograms of $SDDIST\_PROC\_T_{p\_zn}$ values for the time period between the appearance of the vehicle in the controlled area and the disappearance from that area: a) urban buses, b) *other users*, c) vehicles in adjacent traffic lanes

The *PROC* values of variable T_{p_zn} in Figure 16 range from approx. 9.1 % to approx. 11.1 % for the urban operator, approx. 9.0 % to approx. 11.0 % for *other users* and approx. 9.6 % to 10.5 % for vehicles running in adjacent lanes. Lack of agreement between the simulated and measured values was indicated by 5.9 % (urban buses), 3.9 % (*other users*) and 2.4 % (vehicles in adjacent lanes) of simulation results found to be inconsistent with the measurement data. Similar results were obtained in the case of the *SDDIST_PROC* measure (Fig. 17). The largest deviations from the uniform distributions were obtained for vehicles of *other users*, amounting to approx. 9.9 %, while for urban buses, the deviations amounted to 9.4 %, with 3.0 % for vehicles in the adjacent lane to the stop.

Analysis of *PROC* and *SDDIST_PROC* measures for the studied variables shows that the distributions of their values, illustrated by the histograms in Figures 14 to 17, are close to a uniform distribution. It can thus be assumed that the simulated values of the parameters are in agreement with the observed values. The distribution of the analysed measures was found to be in sufficient agreement with the uniform distribution to consider the simulations as good. The biggest differences relative to the uniform distribution were estimated at the level of approx. 10 %.

In addition, the simulation results were analysed individually for each vehicle in order to find the reasons for the lack of agreement between the results. Unscheduled prolonged stops of private busses, related neither to passenger exchange nor to re-entering the traffic stream, as well as unusually long on-board fare collection was observed among the recorded irregularities, not included in the developed simulation model. There were also isolated cases of passing vehicles standing at the stop to occupy the preceding passenger exchange berths. The discrepancies result from the random variability of the empirical and simulation trials/samples.

The traffic flow model between intersections is used to determine the speed of the vehicle, the stopped time due to a queue and the running time along the segment under analysis. It also enables the calculation of the measures of service quality at the stop and the assessment of traffic conditions in its vicinity.

Making changes to the geometry, movement control, and the operation of bus stops and adjacent infrastructure require quantifying anticipated benefits against costs to be incurred. Measures of efficiency are used for this purpose.

In order to verify the developed simulation model in terms of measures for assessing traffic conditions and passenger service quality, the basic parameters of bus stop operation were compared. These were the average delays incurred by buses and other vehicles and their probability levels. Tables C.1 ÷ C.7 (Appendix C) compare the simulated and measured traffic conditions measures by different groups of users: average delays due to a queue before the stop are shown in Tables C.1 and C.2 (Appendix C); average time lost due to obstructed departure from the stop are compiled in Tables C.3 and C.4 (Appendix C); average stop time delays for taxis and other vehicles moving in the lane with the stop, including vehicles making right turns at the intersection downstream of the stop are summarised in Table C.5 (Appendix C); average stop time delay for suburban and intercity buses moving along the lane with the bus stop is shown in Table C.6 (Appendix C); and average delays of vehicles in the lane adjacent to the stop due to merging of buses and other vehicles coming from the stop are in Table C.7 (Appendix C). Delays were calculated as additional dwell time related to a specific type of disturbance. A delay and its probability were determined for affected vehicles and for situations, d_{z2}, in which the bus moves towards the stop exit and stops, blocked by the preceding vehicles, with the rear part of the vehicle still at the stop and partially outside of it.

The model was also verified using the data measured at the bus stops "Warszawska/Politechnika" (KIEL-11), "Urząd Wojewódzki" (KIEL-12), "Galeria Korona" (KIEL-13) and "Warszawska os. Sady" (KIEL-14) in Kielce. These data were excluded from the model development process.

Comparison of the simulated and actual mean values of delay $\bar{d}_z$ shows that the developed simulation model properly represents vehicle movement at and around bus stops used by various users and allows estimation of the basic measures of traffic conditions and service quality. In the case of urban buses, the discrepancies between the simulated and actual values were recorded for bus stops KRAK-04, KRAK-09 and KIEL-01 in Kielce. In these cases, the measured result exceeded the simulated values by 0.1 to 0.5 s/bus.

Discrepancies between the average delays of suburban and intercity buses were recorded for bus stops

KRAK-02 and KIEL-10. The differences were up to 0.3 s/bus relative to the limit values obtained from the simulation.
Urban bus average delays due to the inability to stop at the berth ranged from 0 and 24 s/bus at the delay probability 0 to 44.1 % depending on the bus stop. The simulation runs indicated that due to the randomness of passenger service, parking place selection and other processes, the average delays can reach higher values than those measured, at the same bus and other vehicle arrival sequence maintained. In addition to the random factors, the differences between the measurement and simulation results may also be influenced by other deterministic factors not included in the model.
Under simulated conditions, the average delays due to buses waiting in the queue before the stop reach 26.6 s/bus. The number of suburban and intercity buses experiencing delay in queues is lower (measured: 0 to 21.7 %, simulated: 0 to 26.1 %), which is related to serving passengers on farther positions, also in the queue before the stop. According to the measurements, the average delays d_{z1_z} of suburban and intercity buses reach 33.4 s/bus and up to 34.6 s/bus according to the simulation results.
Average delays d_{z2} due to inability to depart from a stop were experienced by 0 to 68.8% of urban buses (simulation values: 0 to 81.3 %) and 0 to 48.3 % of suburban and intercity buses (simulation values: 0 to 55.2 %). The delays d_{z2_z} of urban buses were up to 35.9 s/bus (simulated value: 34.5 s/bus), while those of suburban and intercity buses reached 29.1 s/A (simulated value: 33.8 s/bus). The measured delays d_{z2} are approximate estimates assumed to occur 8 s (urban buses) and 2 s (suburban and intercity buses) after the completion of passenger service (clearance time).
The calculations included delays of other vehicles moving in the lane with a stop, bus bay and adjacent lane. The results show that the developed simulation model adequately reflects vehicle movement processes at and around bus stops.
The measured delays $\bar{d}_{z\_tds}$ of taxis and other vehicles (Table C.5, Appendix C) moving along the bus stop lane, vehicles turning right at the intersection after leaving the stop were from 0 to 33.3 s/veh (simulated values: 0 up to 35.5 s/veh); the probability of delay occurrence ranged from 0 to 57.1 % (measured) and from 0 to 100 % (simulated).
Delays $\bar{d}_{z\_z}$ (Table C.6, Appendix C) incurred by suburban and intercity buses moving along the lane with a stop, where no passengers were served ranged from 0 to 18.5 s/veh (measured) and from 0 to 20.5 s/veh (simulated), with the probability of additional stopping between 0 and 75 % (measured) and from 0 to 100 % (simulated).
Average delays $\bar{d}_{z\_ps}$ of vehicles in the lane adjacent to the stop (Table C.7, Appendix C), incurred as a result of buses and other vehicles joining the traffic stream from the stop reached 0 to 8.5 s/veh (measured) and 0 to 9.3 s/veh (simulated), with the probability of 0 to 14.1 % (measured) and 0 to 14.9 % (simulated).
For the additional bus stops KIEL-12, KIEL-13, and KIEL-14, whose data were not used in model development, a satisfactory agreement was obtained between the simulated and observed values of the performance indicators, including average delays and the probability of queueing.
As demonstrated, the structure of the developed model allows analysing the effectiveness of various technical and organizational solutions for enhancing the operation of bus stops and adjacent facilities.

7. Summary and conclusions

Performance of bus stops and traffic efficiency in adjacent lanes is strongly dependent on tens of factors related to bus stop/street geometry, vehicle movement, infrastructure, traffic volume, traffic organization and user behaviours. Large numbers of minibuses of non-urban bus carriers stopping at bus stops cause significant disruptions in the traffic flow. The fuzzy logic-based car-following model can be used to characterize the movement of transit vehicles movement at and around urban bus stop used by various bus operators. The selection of the shape of fuzzy sets and membership functions was based on multiple simulation runs. Simulation results were compared with the measured results collected at selected test sites. Statistical tests showed no significant differences between the distribution of real and simulated situations for about half of the test sites under analysis. It was found that one of the reasons for the occurrence of significant discrepancies may be inaccurate lane manoeuvres in the model, in particular in weaving traffic zones and under congestion in neighbouring lanes. This indicates the need to model these processes more accurately in the subsequent stages of model creation.

The developed simulation model was verified and validated in several stages. Initially, the individual sub-models were validated using the Wilcoxon rank-sum test, the PROC and SDDIST measures, with additional validation data from stop KIEL-11 that were not used for model development. The complete model was then verified on traffic performance and service quality measures, such as average delays and queueing probability, showing satisfactory agreement between simulated and observed data. Additional validation performed for bus stops KIEL-12, KIEL-13 and KIEL-14 also demonstrated good consistency of results (Tables C.1–C.7). The positive results confirm that the adopted assumptions and parameters adopted reliably represent the operation of shared use bus stops under heterogeneous and deregulated passenger service conditions. Further research will focus on extended calibration and validation using independent data from other cities to confirm the general applicability of the model under diverse urban traffic conditions.

The initial simulation model was supplemented with components contributing more details, i.e., a passenger service model and algorithms for making a decision to start boarding and alighting passengers, lane changing, and traffic lights system. Two types of lane change were considered, forced lane change and free lane change, including the so-called 'courtesy' braking, making it easier for buses to change lanes in the event of heavy congestion in the adjacent lane. For each simulated vehicle, statistics were calculated for the data obtained from one hundred simulations and auxiliary measures were used, allowing for the interpretation of the simulation results. On the basis of the determined distributions of selected measures, it was found that the simulations accurately reflect the traffic processes in the vicinity of stops used by various users, also for the bus stop that was not used in creating the model. Incidentally occurring dwell time discrepancies between the results of measurements and simulations were due to a conversation with the driver or luggage loading/unloading. These events are difficult to model in the simulation.

The developed and presented model is suitable for the analysis of disruptions and mapping non-typical behaviour of drivers of private carriers. The implementation of subsequent simulation runs using the developed model will allow extending the existing methods of estimating dwell time, bus stop capacity, and the coefficients correcting the capacity of intersections. These extensions may support evaluation of bus transit at bus stops used by various bus operators and efficiency of adjacent infrastructure. Further simulation runs will refine the formulas for calculating efficiency measures.

Despite satisfactory performance and high level of agreement between simulated and observed traffic parameters, the proposed fuzzy logic-based car-following model has several limitations that should be acknowledged. First, the rule-based inference structure and manually calibrated membership functions, although ensuring interpretability and transparency, limit the transferability to other traffic environments without additional recalibration. Moreover, the current version does not account for driver learning effects or adaptive behaviour under prolonged congestion. Second, while the fuzzy logic approach effectively captures heterogeneous and uncertain driver responses, it requires higher computational effort compared with deterministic models such as Gipps or the Intelligent Driver Model (IDM). Third, the model has not yet been benchmarked against hybrid neuro-fuzzy or reinforcement learning (RL) frameworks, which may enhance predictive performance under mixed traffic conditions. These limitations, however, do not affect the validity of the present conclusions, but indicate directions for future work. Future research will include systematic comparison with classical (Gipps, IDM) and hybrid (ANFIS, RL-based) models to evaluate their applicability to shared-use bus stop environments and to quantify trade-offs between interpretability, calibration effort, and computational efficiency.

The modular design of the simulation model makes potential revisions easier. The developed model of the movement of buses and other vehicles within the bus stop area should be further calibrated and validated after adding more detailing components, e.g., using the genetic algorithm method. Extension of this car-following model to include the use of neural-fuzzy systems is worth considering.

References

1. Adamski, A. (1992). Probabilistic models of passengers service processes at bus stops. *Transportation Research Part B: Methodological*, 26, 253–259. https://doi.org/10.1016/0191-2615(92)90036-V.
2. Ahmed, H. U., Huang, Y., & Lu, P. (2021). A review of car-following models and modeling tools for human and autonomous-ready driving behaviors in micro-simulation. *Smart Cities*, 4, 314–335. https://doi.org/10.3390/smartcities4010019.
3. Alonso, B., Moura, J. L., Ibeas, A., & Dell'Olio, L. (2013). Analytical model for calibrating delay at congested bus stops. *Transport Planning and Technology*, 36, 520–528. https://doi.org/10.1080/03081060.2013.830893.
4. Bąk, R. (2010). Simulation model of the bus stop. *Archives of Transport*, 1, 5–25.
5. Bando, M., Hasebe, K., Nakanishi, K., Nakayama, A., Shibata, A., & Sugiyama, Y. (1995). Dynamical model of traffic congestion and numerical simulation. *Physical Review* E, 51, 1035–1042. https://doi.org/10.1103/PhysRevE.51.1035.
6. Bauer, M., Dźwigoń, W., Richter, M. (2021). Personal Safety of Passengers during the First Phase Covid-19 Pandemic in the Opinion of Public Transport Drivers in Krakow. *Archives of Transport*, *59*, 41–55, https://doi:10.5604/01.3001.0015.0090.
7. Benekohal, R. F., & Treiterer, J. (1988). CARSIM: Car-following model for simulation of traffic in normal and stop-and-go conditions. *Transportation Research Record*, 1194, 99–111.
8. Berrebi, S. J., Watkins, K. E., & Laval, J. A. (2015). A real-time bus dispatching policy to minimize passenger wait on a high frequency route. *Transportation Research Part B: Methodological*, 81, 377–389. https://doi.org/10.1016/j.trb.2015.05.012.
9. Carrillo-González, J. G., López-Ortega, J., Sandoval-Gutiérrez, J., & Perez-Martinez, F. (2021). Impact of buses, taxis, passenger cars, and traffic infrastructure on average travel speed. *Journal of Advanced Transportation*, 2021, 1–10. https://doi.org/10.1155/2021/8883068.
10. Chakroborty, P., & Kikuchi, S. (2003). Calibrating the membership functions of the fuzzy inference system: Instantiated by car-following data. *Transportation Research Part C: Emerging Technologies*, 11, 91–119. https://doi.org/10.1016/S0968-090X(02)00022-0.
11. Chandler, R. E., Herman, R., & Montroll, E. W. (1958). Traffic dynamics: Studies in car following. *Operations Research*, 6, 165–184. https://doi.org/10.1287/opre.6.2.165.
12. Chomicz-Kowalska, A., & Stępień, J. (2016). Cost and eco-effective cold in-place recycled mixtures with foamed bitumen during the reconstruction of a road section under variable load bearing capacity of the subgrade. *Procedia Engineering*, 161, 980–989. https://doi.org/10.1016/j.proeng.2016.08.837.
13. Cingel, M, Drliciak, M., Celko, J. (2021). Morning modal split model of economically active people in Zilina Region. *Transportation Research Procedia*, 55, 1065–1072, https://doi:10.1016/j.trpro.2021.07.077.
14. Drabicki, A. A., Islam, M. F., & Szarata, A. (2021). Investigating the impact of public transport service disruptions upon passenger travel behaviour—Results from Krakow City. *Energies, 14*, 4889. https://doi.org/10.3390/en14164889.
15. European Commission. (2020). Sustainable and smart mobility strategy – Putting European transport on track for the future. Available online: https://eur-lex.europa.eu/legal-content/EN/TXT/?uri=CELEX:52020DC0789 (accessed 27 October 2025).
16. European Commission. (2021). The New EU Urban Mobility Framework. Available online: https://eur-lex.europa.eu/legal-content/EN/TXT/?uri=CELEX:52021DC0811 (accessed 27 October 2025).
17. European Commission. (2023). Guidelines for Developing and Implementing a Sustainable Urban Mobility Plan (2nd Edition). Available online: https://urban-mobility-observatory.transport.ec.europa.eu/system/files/2023-09/sump_guidelines_2019_second%20edition.pdf (accessed 27 October 2025).
18. Faron, A. (2018). Spatial development city models in transport sustainable mobility issue. *Proceedings Paper. International Multidisciplinary Scientific GeoConference-SGEM.*, 18, https://doi.org/10.5593/sgem2018V/6.4/S10.100.

19. Feng, Y., Iravani, P., & Brace, C. (2021). A fuzzy logic-based approach for humanized driver modelling. *Journal of Advanced Transportation*, 2021, 1–13. https://doi.org/10.1155/2021/4413505.
20. Feng, Y., Pickering, S., Chappell, E., Iravani, P., & Brace, C. (2019). Driving style modelling with adaptive neuro-fuzzy inference system and real driving data. *Advances in Intelligent Systems and Computing*, (pp. 481–490). https://doi.org/10.1007/978-3-319-93885-1_43.
21. Fernández, R. (2010). Modelling public transport stops by microscopic simulation. *Transportation Research Part C: Emerging Technologies*, 18, 856–868. https://doi.org/10.1016/j.trc.2010.02.002.
22. Fitzová, H., & Matulová, M. (2020). Comparison of urban public transport systems in the Czech Republic and Slovakia: Factors underpinning efficiency. *Research in Transportation Economics*, 81, 100824. https://doi.org/10.1016/j.retrec.2020.100824.
23. Fritzsche, H.-T. (1994). A model for traffic simulation. *Traffic Engineering & Control*, 35, 317–321.
24. Gipps, P. G. (1981). A behavioural car-following model for computer simulation. Transportation Research Part B: Methodological, 15, 105–111. https://doi.org/10.1016/0191-2615(81)90037-0.
25. Gu, W., Cassidy, M. J., & Li, Y. (2015). Models of bus queueing at curbside stops. *Transportation Science,* 49, 204–212. https://doi.org/10.1287/trsc.2014.0537.
26. Gu, W., Cassidy, M. J., Gayah, V. V., & Ouyang, Y. (2013). Mitigating negative impacts of near-side bus stops on cars. *Transportation Research Part B: Methodological*, 47, 42–56. https://doi.org/10.1016/j.trb.2012.09.005.
27. Hansson, J., Pettersson, F., Svensson, H., & Wretstrand, A. (2019). Preferences in regional public transport: A literature review. *European Transport Research Review*, 11, 38. https://doi.org/10.1186/s12544-019-0374-4.
28. Hu, S., Shen, M., & Gu, W. (2023). Impacts of bus overtaking policies on the capacity of bus stops. *Transportation Research Part A: Policy and Practice*, 173, 103702. https://doi.org/10.1016/j.tra.2023.103702.
29. Ištoka Otković, I., Tollazzi, T., Šraml, M., & Varevac, D. (2023). Calibration of the microsimulation traffic model using different neural network applications. *Future Transportation*, 3, 150–168. https://doi.org/10.3390/futuretransp3010010.
30. Jin, H., Liu, Y., Wu, T., & Zhang, Y. (2022). Site-specific optimization of bus stop locations and designs over a corridor. *Physica A: Statistical Mechanics and Its Applications*, 599, 127441. https://doi.org/10.1016/j.physa.2022.127441.
31. Jin, H., Yu, J., & Yang, X. (2019). Impact of curbside bus stop locations on mixed traffic dynamics: A bus route perspective. *Transportmetrica A: Transport Science*, 15, 1419–1439. https://doi.org/10.1080/23249935.2019.1601789.
32. Jinxing, S., Feng, Q., Rui, L., & Changjiang, Z. (2017). An extended car-following model considering the influence of bus. Tehnički Vjesnik – *Technical Gazette*, 24. https://doi.org/10.17559/TV-20170317215248.
33. Jovanović, A., & Teodorović, D. (2022). Type-2 fuzzy logic based transit priority strategy. *Expert Systems with Applications*, 187, 115875. https://doi.org/10.1016/j.eswa.2021.115875.
34. Joyce, P., & Yagar, S. (1990). Representing stochastic transit dwell times in traffic signal optimization. *Transportation Research Part A: General*, 24, 87–98. https://doi.org/10.1016/0191-2607(90)90016-Y.
35. Khodayari, A., Ghaffari, A., Kazemi, R., & Braunstingl, R. (2012). A modified car-following model based on a neural network model of the human driver effects. *IEEE Transactions on Systems, Man, and Cybernetics – Part A: Systems and Humans*, 42, 1440–1449. https://doi.org/10.1109/TSMCA.2012.2192262.
36. Khodayari, A., Kazemi, R., Ghaffari, A., & Braunstingl, R. (2011). Design of an improved fuzzy logic-based model for prediction of car following behavior. *In Proceedings of the 2011 IEEE International Conference on Mechatronics* (pp. 200–205). IEEE. https://doi.org/10.1109/ICMECH.2011.5971281.
37. Kim, M. (Edward), Levy, J., & Schonfeld, P. (2019). Optimal zone sizes and headways for flexible-route bus services. *Transportation Research Part B: Methodological*, 130, 67–81. https://doi.org/10.1016/j.trb.2019.10.006.

38. Kosko, B. (1994). Fuzzy systems as universal approximators. *IEEE Transactions on Computers*, 43, 1329–1333. https://doi.org/10.1109/12.324566.
39. Krivda, V., Petru, J., Macha, D., & Novak, J. (2021). Use of microsimulation traffic models as means for ensuring public transport sustainability and accessibility. *Sustainability*, 13, 2709. https://doi.org/10.3390/su13052709.
40. Krystek, R. (1980). Symulacja ruchu potoku pojazdów [Simulation of traffic flow]. WKŁ: Warsaw.
41. Kwesiga, D. K., Guin, A., & Hunter, M. (2025). Analysis of bus dwell times from automated passenger count data and the impact of dwell-time variability on the performance of transit signal priority. *Public Transport*. https://doi.org/10.1007/s12469-025-00393-y.
42. Lee, S.-Y., & Le, T. H. M. (2023). Evaluating pavement performance in bus rapid transit systems: Lessons from Seoul, South Korea. *Case Studies in Construction Materials*, 18, e02065. https://doi.org/10.1016/j.cscm.2023.e02065.
43. Leungbootnak, N., Li, Z., Wei, Z., Lord, D., & Zhang, Y. (2025). Modeling headway in heterogeneous and mixed traffic flow: A statistical distribution based on a general exponential function. arXiv preprint. https://doi.org/10.48550/arXiv.2511.03154.
44. Li, L., Yang, S., & Cao, W. (2014). Driver's speed decision-making model based on ANFIS. *Applied Mechanics and Materials,* 488–489, 955–960. https://doi.org/10.4028/www.scientific.net/AMM.488-489.955.
45. Li, R., Yang, Q., Qi, T., & Xue, X. (2023). Simulation analysis of capacity evaluation of bus stops under connected and automated vehicles environment. *Applied Sciences*, 13, 9186. https://doi.org/10.3390/app13169186.
46. Liu, J., Jiang, R., Zhao, J., & Shen, W. (2023). A quantile-regression physics-informed deep learning for car-following model. *Transportation Research Part C: Emerging Technologies*, 154, 104275. https://doi.org/10.1016/j.trc.2023.104275.
47. Liu, L., Bian, Z., & Nie, Q. (2022). Finding the optimal bus-overtaking rules for bus stops with two tandem berths. *Sustainability*, 14, 5343. https://doi.org/10.3390/su14095343.
48. Ma, L., & Qu, S. (2020). A sequence-to-sequence learning based car-following model for multi-step predictions considering reaction delay. *Transportation Research Part C: Emerging Technologies*, 120, 102785. https://doi.org/10.1016/j.trc.2020.102785.
49. Ma, X. (2006). A neural-fuzzy framework for modeling car-following behavior. In *Proceedings of the 2006 IEEE International Conference on Systems, Man and Cybernetics* (pp. 1178–1183). IEEE. https://doi.org/10.1109/ICSMC.2006.384560.
50. Meng, Q., & Qu, X. (2013). Bus dwell time estimation at bus bays: A probabilistic approach. *Transportation Research Part C: Emerging Technologies*, 36, 61–71. https://doi.org/10.1016/j.trc.2013.08.007.
51. Milla, F., Saez, D., Cortes, C. E., & Cipriano, A. (2012). Bus-stop control strategies based on fuzzy rules for the operation of a public transport system. *IEEE Transactions on Intelligent Transportation Systems*, 13, 1394–1403. https://doi.org/10.1109/TITS.2012.2188394.
52. Mo, Z., Shi, R., & Di, X. (2021). A physics-informed deep learning paradigm for car-following models. Transportation *Research Part C: Emerging Technologies*, 130, 103240. https://doi.org/10.1016/j.trc.2021.103240.
53. Naghawi, H., Shattal, M. A., & Idewu, W. (2019). Application of AIMSUN microscopic simulation model in evaluating side friction impacts on traffic stream performance. *International Journal of Transport and Vehicle Engineering*, 13. https://doi.org/10.5281/zenodo.3607767.
54. Ngoduy, D., & Li, T. (2021). Hopf bifurcation structure of a generic car-following model with multiple time delays. *Transportmetrica A: Transport Science*, 17, 878–896. https://doi.org/10.1080/23249935.2020.1818002.
55. Panwai, S., & Dia, H. (2005). Comparative evaluation of microscopic car-following behavior. *IEEE Transactions on Intelligent Transportation Systems*, 6, 314–325. https://doi.org/10.1109/TITS.2005.853705.

56. Phillips, R. O., Hagen, O. H., & Berge, S. H. (2021). Bus stop design and traffic safety: An explorative analysis. *Accident Analysis & Prevention*, 153, 105917. https://doi.org/10.1016/j.aap.2020.105917.
57. Pojani, D., & Stead, D. (2015). Sustainable urban transport in the developing world: Beyond megacities. *Sustainability*, 7, 7784–7805. https://doi.org/10.3390/su7067784.
58. PTV Group. (2025). PTV Vissim 2025 User Manual.
59. Raj, P., Asaithambi, G., & Ravi Shankar, A. U. (2022). Effect of curbside bus stops on passenger car units and capacity in disordered traffic using simulation model. *Transport Letters*, 14, 104–113. https://doi.org/10.1080/19427867.2020.1815145.
60. Rudnicki, A. (1977). Symulacja funkcjonowania przystanku autobusowego [Simulation of the Functioning of a Bus Stop]. *Archiwum Inżynierii Lądowej*, 1.
61. Sangole, J. P., & Patil, G. R. (2014). Adaptive neuro-fuzzy inference system for gap acceptance behavior of right-turning vehicles at partially controlled T-intersections. *Journal of Modern Transportation*, 22, 235–243. https://doi.org/10.1007/s40534-014-0057-8.
62. Shen, M., Gu, W., & Hu, S. (2019). Capacity approximations for near- and far-side bus stops in dedicated bus lanes. *Transportation Research Part B: Methodological*, 125, 94–120. https://doi.org/10.1016/j.trb.2019.04.010.
63. Śleszyński, P., Olszewski, P., Dybicz, T., Goch, K., & Niedzielski, M. A. (2023). The ideal isochrone: Assessing the efficiency of transport systems. *Research in Transportation Business & Management*, 46, 100779. https://doi.org/10.1016/j.rtbm.2021.100779.
64. Stępień, J. (2017). Wpływ przystanków autobusowych na sprawność ruchu drogowego i komunikacji miejskiej [The Impact of Bus Stops on the Efficiency of Road Traffic and Urban Public Transport]. Doctoral dissertation. Kielce University of Technology.
65. Takagi, T., & Sugeno, M. (1985). Fuzzy identification of systems and its applications to modeling and control. *IEEE Transactions on Systems, Man and Cybernetics*, SMC-15, 116–132. https://doi.org/10.1109/TSMC.1985.6313399.
66. Taylor, Z., & Ciechański, A. (2018). Systemic transformation and changes in surface transport companies in Poland: A synthesis after twenty-five years. *Journal of Transport Geography*, 70, 114–122. https://doi.org/10.1016/j.jtrangeo.2018.05.016.
67. Tian, L. (2012). Traffic flow simulation in a scenario with signalized intersection and bus stop. *Journal of Transportation Systems Engineering and Information Technology*, 12, 90–96. https://doi.org/10.1016/S1570-6672(11)60226-2.
68. Tirachini, A., Hensher, D. A., & Rose, J. M. (2014). Multimodal pricing and optimal design of urban public transport: The interplay between traffic congestion and bus crowding. *Transportation Research Part B: Methodological*, 61, 33–54. https://doi.org/10.1016/j.trb.2014.01.003.
69. Toan, T. D., & Wong, Y. D. (2021). Fuzzy logic-based methodology for quantification of traffic congestion. *Physica A: Statistical Mechanics and Its Applications*, 570, 125784. https://doi.org/10.1016/j.physa.2021.125784.
70. Treiber, M., & Kesting, A. (2013). Traffic Flow Dynamics (1st ed.). *Data, Models and Simulation*. Springer Berlin, Heidelberg, https://doi.org/10.1007/978-3-642-32460-4.
71. Tunc, I., & Soylemez, M. T. (2023). Fuzzy logic and deep Q-learning based control for traffic lights. *Alexandria Engineering Journal*, 67, 343–359. https://doi.org/10.1016/j.aej.2022.12.028.
72. Tunc, I., Yesilyurt, A. Y., & Soylemez, M. T. (2021). Different fuzzy logic control strategies for traffic signal timing control with state inputs. *IFAC-PapersOnLine*, 54, 265–270. https://doi.org/10.1016/j.ifacol.2021.06.032.
73. van Hinsbergen, C. P. I. J., Schakel, W. J., Knoop, V. L., van Lint, J. W. C., & Hoogendoorn, S. P. (2015). A general framework for calibrating and comparing car-following models. *Transportmetrica A: Transport Science*, 11, 420–440. https://doi.org/10.1080/23249935.2015.1006157.
74. Vatchova, B., Boneva, Y., & Gegov, A. (2023). Modelling and simulation of traffic light control. *Cybernetics and Information Technologies*, 23, 179–191. https://doi.org/10.2478/cait-2023-0032.
75. Wang, C., Ye, Z., Chen, E., & Xu, M. (2019). Diffusion approximation for exploring the correlation

between failure rate and bus-stop operation. *Transportmetrica A: Transport Science*, 15, 1306–1320. https://doi.org/10.1080/23249935.2019.1594445.
76. Wang, C., Ye, Z., Wang, Y., Xu, Y., & Wang, W. (2016). Modeling bus dwell time and time lost serving stop in China. *Journal of Public Transportation*, 19, 55–77. https://doi.org/10.5038/2375-0901.19.3.4.
77. Wang, T., Huang, L., Tian, J., Zhang, J., Yuan, Z., Zheng, J. (2024). Bus dwell time estimation and overtaking maneuvers analysis: A stochastic process approach. *Transportation Research Part E: Logistics and Transportation Review*, 186, 103577. https://doi.org/10.1016/j.tre.2024.103577.
78. Wang, X., Jiang, R., Li, L., Lin, Y.-L., & Wang, F.-Y. (2019). Long memory is important: A test study on deep-learning based car-following model. *Physica A: Statistical Mechanics and Its Applications*, 514, 786–795. https://doi.org/10.1016/j.physa.2018.09.136.
79. Wang, Z., Huang, H., Tang, J., Meng, X., & Hu, L. (2022). Velocity control in car-following behavior with autonomous vehicles using reinforcement learning. *Accident Analysis & Prevention*, 174, 106729. https://doi.org/10.1016/j.aap.2022.106729.
80. Xu, L., Ma, J., & Wang, Y. (2022). A car-following model considering the effect of following vehicles under the framework of physics-informed deep learning. *Journal of Advanced Transportation*, 2022, 1–12. https://doi.org/10.1155/2022/3398862.
81. Xue, Y., Zhong, M., Xue, L., Zhang, B., Tu, H., Tan, C., Kong, Q., & Guan, H. (2022). Simulation analysis of bus passenger boarding and alighting behavior based on cellular automata. *Sustainability*, 14, 2429. https://doi.org/10.3390/su14042429.
82. Yang, X., Liu, Z., Cheng, Q., & Liu, P. (2024). Geometry-aware car-following model construction: Theoretical modeling and empirical analysis on horizontal curves. *Transportation Research Part C: Emerging Technologies*, 166, 104772. https://doi.org/10.1016/j.trc.2024.104772.
83. Zhang, J., Li, Z., Zhang, F., Qi, Y., Zhou, W., Wang, Y., Zhao, D., & Wang, W. (2018). Evaluating the impacts of bus stop design and bus dwelling on operations of multitype road users. *Journal of Advanced Transportation*, 2018, 1–10. https://doi.org/10.1155/2018/4702517.
84. Zhang, Y., Shao, Y., Shi, X., & Ye, Z. (2024). A testing and evaluation method for the car-following models of automated vehicles based on driving simulator. *Systems*, 12, 298. https://doi.org/10.3390/systems12080298.
85. Zhao, X., Gao, Z., & Jia, B. (2007). The capacity drop caused by the combined effect of the intersection and the bus stop in a CA model. *Physica A: Statistical Mechanics and Its Applications*, 385, 645–658. https://doi.org/10.1016/j.physa.2007.07.040.
86. Zhao, X., Gao, Z., & Li, K. (2008). The capacity of two neighbour intersections considering the influence of the bus stop. *Physica A: Statistical Mechanics and Its Applications*, 387, 4649–4656. https://doi.org/10.1016/j.physa.2008.03.011.
87. Zheng, P., & McDonald, M. (2005). Application of fuzzy systems in the car-following behaviour analysis. *Lecture Notes in Computer Science*. (pp. 782–791). https://doi.org/10.1007/11539506_97.
88. Zhenyu, L., & Meiying, J. (2019). Traffic impacts analysis of bus stops near signalized intersections based on an optimal velocity model. *Advances in Mechanical Engineering*, 11. https://doi.org/10.1177/1687814019848272.
89. Zhou, X., Guo, H., Li, B., & Zhao, X. (2024). Transit dynamic operation optimization using combination of stop-skipping strategy and local route optimization. *Applied Sciences*, 14, 7783. https://doi.org/10.3390/app14177783.
90. Zhu, K., Zhang, Y., Wang, H., Chen, L., & Zhang, X. (2024). A heterogeneity-aware car-following model: Based on mixed vehicle traffic flow. *Algorithms*, 17, 68. https://doi.org/10.3390/a17020068.

Appendix A. Comparison of the state of research

Table A.1. Comparison of key car-following models, fuzzy-logic-based approaches, and simulation tools (CF – car-following, PT- public transport, AV/HDV - autonomous vehicle / human-driven vehicle, ANFIS - adaptive neuro-fuzzy inference System, RL - reinforcement learning)

Model/study	Method/ approach/data source	Application context	Advantages	Limitations	Relevance to bus or stop operation
Fritzsche (1994)	Psycho-physical (Action Point) model (empirical)	Driver response	Realistic thresholds	No stochasticity	No – general driver response model, not bus-specific
Panwai and Dia (2005)	Comparative evaluation of microscopic CF models (empirical and simulation)	Model validation	Objective comparison	No new model	No – urban car-traffic validation only
L. Li, Yang, and Cao (2014)	ANFIS for speed decision-making (NGSIM trajectory data)	Mixed traffic, CF / free-travel transitions	Captures driver decision-making under uncertainty	Focuses on speed decisions, not full CF interaction modelling	Partial – applicable to mixed traffic, not to stop operations
Sangole and Patil (2014)	ANFIS for gap acceptance at partially controlled T-intersections (field data)	Urban heterogeneous traffic	Realistic modelling of driver decision behaviour	Not directly CF	Partial – models heterogeneous driving, but not bus stops
van Hinsbergen et al. (2015)	Bayesian calibration and comparison framework (empirical trajectories)	Model estimation	Statistical reliability	Requires large datasets	No – statistical calibration framework only
Jinxing et al. (2017)	ANFIS with real driving data (naturalistic data)	Driving style modelling	Adaptivity to driver type	Complex rule structure	Partial – includes buses in naturalistic data but no stop operation
L. Ma and Qu (2020)	Sequence-to-sequence learning with reaction delay (trajectory data)	Multi-step prediction	Considers driver delay	Requires large datasets	No – predictive AI car-following, unrelated to bus stops
Ahmed, Huang, and Lu (2021)	Review of CF models and tools (Vissim, Aimsun, Sumo) (literature)	Mixed human/ autonomous driving	Comprehensive overview	No original modelling	Partial – reviews CF tools including PT modules (e.g.,Vissim)
Mo, Shi, and Di (2021)	Sequence-to-sequence learning with reaction delay (trajectory data)	Multi-step prediction	Considers driver delay	Requires large datasets	No – generic car-following learning framework
Ngoduy and Li (2021)	Bifurcation structure of CF model with delays (analytical)	Mixed traffic	Explains instability	No empirical validation	No – theoretical traffic stability analysis
Xu, Ma, and Wang (2022)	Physics-informed deep learning model (simulation)	AV/mixed traffic	Physics-consistent ML	Limited transparency	No – AV-oriented; no bus or stop component
Jovanović and Teodorović (2022)	Type-2 fuzzy-logic-based transit priority strategy (simulation)	Urban signalized corridors	Advanced fuzzy control integrating uncertainty in transit priority decisions	Focused on intersections; not bus-stop operation	Partial – focuses on transit signal priority, not stop operation
J. Liu et al. (2023)	Quantile-regression physics-informed deep learning (field trajectories)	Mixed traffic	Robust prediction	Lacks interpretability	No – general mixed-traffic prediction model
Tunc and Soylemez (2023)	Hybrid deep Q-Learning and fuzzy logic for traffic-signal control (simulation)	Urban intersections	Integrates RL and Fuzzy Logic for adaptive signal timing	Not bus-stop-specific	No – signal control only; unrelated to stop behaviour
X. Yang et al. (2024)	Geometry-aware CF model (field and simulation data)	Curved road segments	Considers geometric road curvature in CF behaviour	Deterministic, not fuzzy-based	No – geometric CF model without PT elements

Model/study	Method/ approach/data source	Application context	Advantages	Limitations	Relevance to bus or stop operation
Y. Zhang et al. (2024)	Testing and evaluation framework for CF models includes fuzzy reasoning model (driving simulator data)	Mixed HDV/AV scenarios	Comprehensive validation of multiple CF models, including fuzzy logic	Focused on testing environment, not model development	Partial – includes fuzzy reasoning, but not bus-stop application

Table A.2. Comparison of key microscopic simulation models of bus stop operation and their relevance to shared-use, unregulated passenger service conditions (CAV - connected and autonomous vehicles, APC - automated passenger count, TSP - transit signal priority, CA - cellular automata, PT - public transport)

Model/study	Method/ approach/data source	Application context	Advantages	Limitations	Relevance to this study
Tian (2012)	CA simulation of vehicle movement near a signalised intersection and adjacent bus stop	Urban road section with mixed traffic	Integrates bus dwelling effects with surrounding traffic; early combined stop–traffic model	Discrete CA rules; no continuous car-following logic; simplified passenger and fleet representation	Relevant precursor — captures bus-related traffic interference, though without fuzzy or probabilistic elements
Milla et al. (2012)	Fuzzy-logic-based control strategies for bus headway regularity (simulation)	Urban bus corridors	Demonstrates effective fuzzy control for maintaining headway stability and reducing bunching	Focused on headway regulation; no microscopic passenger or mixed-traffic modelling	Provides methodological reference for fuzzy-based regulation mechanisms
C. Wang et al. (2016)	Empirical decomposition of dwell time and "time lost serving stop" (field data)	Urban bus stops	Field-validated breakdown of operational time components	Deterministic approach; no stochastic passenger process	Empirical basis for modelling passenger-service duration
Xue et al. (2022)	CA-based simulation of bus-passenger boarding / alighting (empirical calibration)	Urban bus stops	Detailed microscopic representation of passenger interactions during boarding / alighting	Limited to passenger flow; no vehicle movement or traffic interaction	Complements the passenger-service component of the proposed integrated model
R. Li et al. (2023)	Microsimulation of bus-stop capacity under CAV scenarios	Urban and CAV conditions	Integrates car-following and lane-change logic near stops	Ordered scenarios; limited heterogeneity	Benchmark for advanced-vehicle capacity evaluation
Zhou et al. (2024)	Stop-skipping and local route optimization using simulation	Urban transit routes	Combines operational and route-level optimization	Focused on system-level efficiency	Complements operational-strategy context
Kwesiga, Guin, and Hunter (2025)	Statistical and APC-based analysis of dwell-time variability and TSP impact	Urban PT network	Real APC dataset; quantifies dwell-time effects on transit-signal performance	Macroscopic scale; no vehicle interactions	Provides empirical background on dwell-time variability

Appendix B. Flowcharts illustrate the traffic situation of buses and other types of vehicles moving in the simulation area

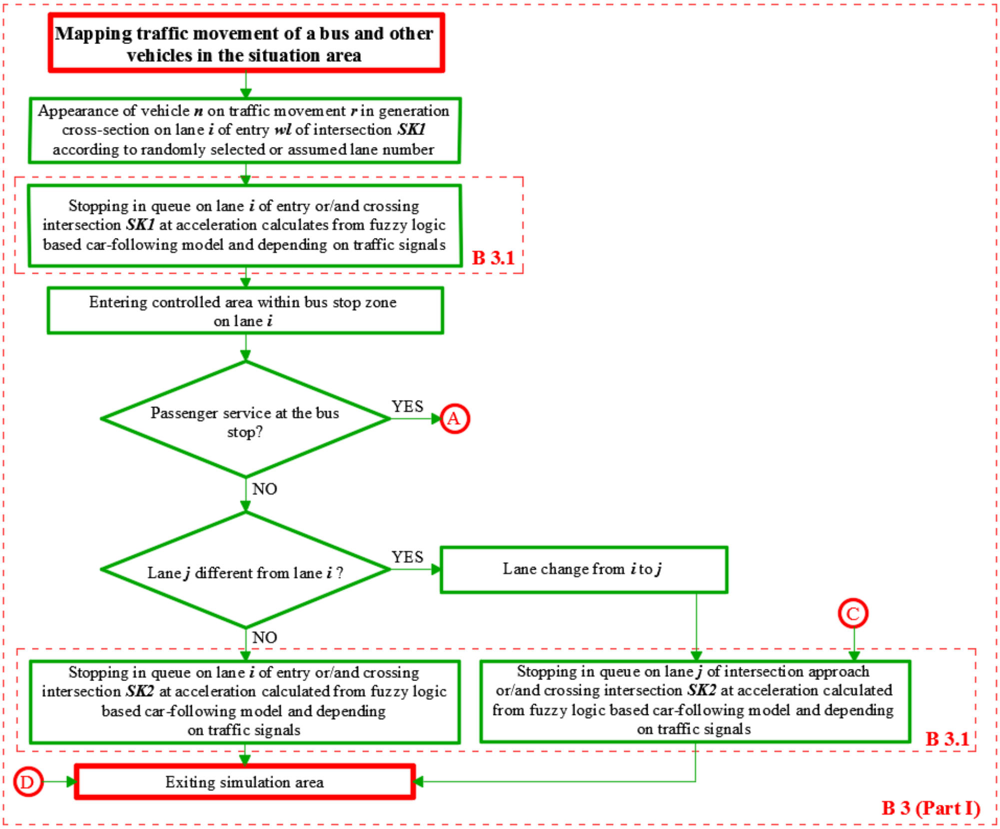

Figure B.1. Scheme of block B3 – analysis of traffic/movement conditions for the vehicle in the simulation area (part I): i – the ID number of the lane on which the vehicle enters the controlled area, j – the ID number of the lane on which the vehicle leaves the controlled area

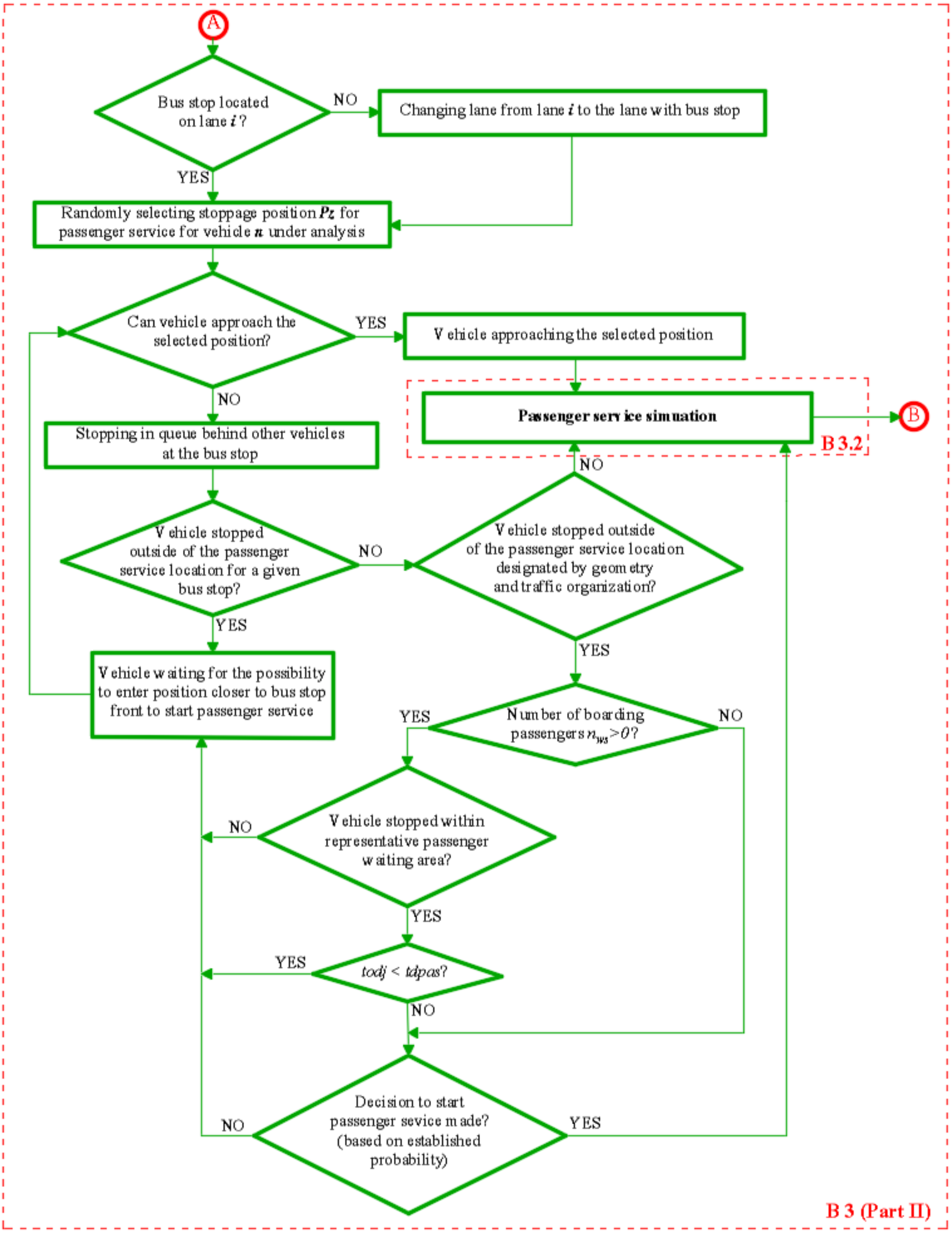

Figure B.2. Scheme of block B3 – analysis of traffic/movement conditions for the vehicle in the simulation area (part II): i – the ID number of the lane on which the vehicle enters the controlled area, j – the ID number of the lane on which the vehicle leaves the controlled area

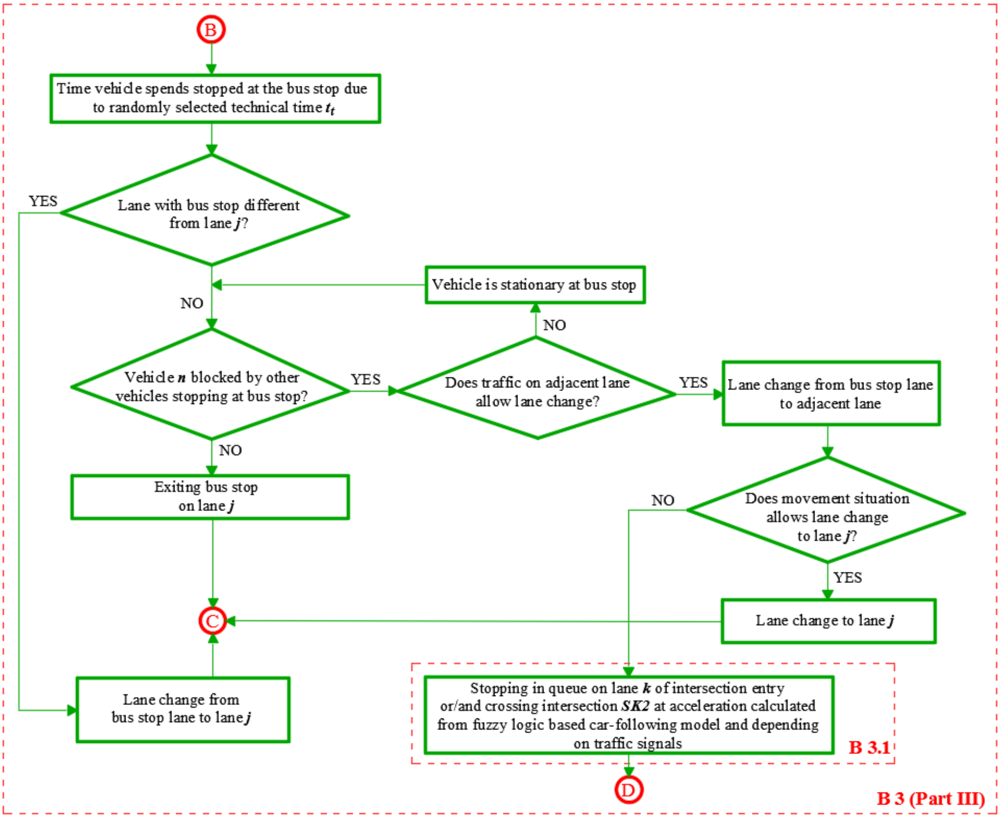

Figure B.3. Scheme of block B3 – analysis of traffic/movement conditions for the vehicle in the simulation area (part III): i – the ID number of the lane on which the vehicle enters the controlled area, j – the ID number of the lane on which the vehicle leaves the controlled area, k – the lane other than i or j

Appendix C. Comparison of simulated and measured traffic conditions measures by different groups of users: average delays due to a queue before the stop

Table C.1. Comparison of simulated and measured average delays for urban buses queueing before the stop

Test site (bus stop)	Average delays incurred by urban buses in the queue before the stop $dz1\_m$ (s/bus)				Probability of queueing before the stop due to obstructed stopping position by the preceding urban buses P_{dz1_m} (%)			
	Measurement	Simulation			Measurement	Simulation		
		Min.	Mean	Max.		Min.	Mean	Max.
KRAK-01	22.0	19.2	23.2	26.2	25.0	17.5	25.0	30.0
KRAK-02	9.5	5.8	8.3	10.8	13.5	7.7	13.5	19.2
KRAK-03	13.9	11.3	14.1	15.9	20.5	12.8	23.1	28.2
KRAK-04	23.5	17.2	21.7	23.0	44.1	32.4	32.4	38.2
KRAK-05	12.8	10.1	13.0	15.9	19.4	13.9	22.2	27.8
KRAK-051	16.9	14.2	16.5	18.8	38.2	29.4	32.4	41.2
KRAK-06	11.8	8.2	10.8	13.3	10.3	3.4	6.9	10.3
KRAK-07	3.0	1.4	2.5	3.3	9.1	0	4.5	9.1
KRAK-08	10.3	9.9	11.1	12.1	20.0	10.0	20.0	26.7
KRAK-09	14.5	13.1	14.8	16.2	20.0	15.5	22.2	26.7
KRAK-091	6.0	6.1	7.2	9.1	6.8	9.1	11.4	13.6
KIEL-01	10.0	6.9	8.5	9.7	5.0	0	5.0	10.0
KIEL-02	8.0	7.2	9.2	11.1	4.8	0	4.8	9.5
KIEL-03	24.0	22.0	24.7	26.6	12.5	6.3	18.8	25.0
KIEL-04	4.0	2.8	4.4	5.2	7.1	7.1	14.3	21.0
KIEL-05	3.0	2.9	4.3	5.5	5.9	5.9	11.8	18.0
KIEL-06	19.0	16.1	18.7	21.2	4.2	0	4.2	8.0
KIEL-07	0	0	1.5	2.1	0	0	5.0	10.0
KIEL-08	0	0	0.8	1.9	0	0	8.3	17.0
KIEL-09	8	6.5	7.2	9.0	8.3	0	8.3	17.0
KIEL-10	18.0	13.8	17.0	19.7	13.3	7.7	13.3	23.0
KIEL-11	5.0	3.0	4.8	6.5	3.7	0	3.8	10.2
KIEL-12	4.0	0	4.5	5.0	1.4	0	2.5	8.1
KIEL-13	6.0	1.5	5.7	7.2	3.5	1.8	4.3	6.1
KIEL-14	6.5	0.9	7.2	9.1	4.2	2.1	6.3	8.4

Table C.2. Comparison of simulated and measured average delays for suburban and intercity buses queueing before the stop

Test site (bus stop)	Average delays incurred by suburban and intercity buses in the queue before the stop $\bar{d}_{z1\_z}$ (s/bus)				Probability of queueing before the stop as a result of service berths taken by the preceding suburban and intercity buses P_{dz1_z} (%)			
	Measurement	Simulation			Measurement	Simulation		
		Min.	Mean	Max.		Min.	Mean	Max.
KRAK-01	19.8	17.7	19.1	22.8	16.3	12.2	16.3	24.5
KRAK-02	12.3	8.3	10.9	12.2	2.4	0	2.4	9.8
KRAK-03	10.3	7.5	10.0	11.8	10.2	6.1	8.2	18.4
KRAK-04	22.7	19.2	21.9	24.3	21.7	18.8	20.3	26.1
KRAK-05	15.9	12.6	15.0	17.4	10.0	5.0	10.0	17.5
KRAK-051	33.4	29.8	32.2	34.6	9.5	6.3	7.9	14.3
KRAK-06	4.5	1.5	3.8	6.3	4.3	0	2.1	8.5
KRAK-07	0	0	1.0	2.0	0	0	1.5	4.5
KRAK-08	5.5	2.7	5.0	7.5	7.5	5.0	6.3	11.3
KRAK-09	13.1	10.4	12.7	15.2	5.6	2.8	4.2	8.3

Test site (bus stop)	Average delays incurred by suburban and intercity buses in the queue before the stop $\bar{d}_{z1\_z}$ (s/bus)				Probability of queueing before the stop as a result of service berths taken by the preceding suburban and intercity buses P_{dz1_z} (%)			
	Measurement	Simulation			Measurement	Simulation		
		Min.	Mean	Max.		Min.	Mean	Max.
KRAK-091	23.3	20.4	22.5	25.2	2.7	0	2.7	8.1
KIEL-01	0	0	0.5	1.0	0	0	2.8	5.6
KIEL-02	0	0	1.0	1.5	0	0	2.9	5.7
KIEL-03	10.0	6.8	9.0	11.6	3.4	0	3.4	6.9
KIEL-04	6.0	2.7	5.1	7.5	3.2	0	3.2	6.5
KIEL-05	2.0	0	1.5	4.1	5.0	0	5.0	10.0
KIEL-06	0	0	1.0	2.5	0	0	5.3	10.5
KIEL-07	0	0	0.6	1.3	0	0	7.7	15.4
KIEL-08	0	0	0.4	1.0	0	0	3.6	7.1
KIEL-09	0	0	0.3	1.0	0	0	7.7	15.4
KIEL-10	4.0	0.8	2.9	3.9	3.6	0	3.6	7.1
KIEL-11	0	0	1.0	2.0	0	0	3.7	11.1
KIEL-12	2.0	0	2.0	4.1	4.5	0	4.5	9.0
KIEL-13	0	0	2.5	4.5	0	0	11.1	22.2
KIEL-14	0	0	3.0	5.1	0	0	14.2	28.4

Table C.3. Comparison of simulated and measured average delays for urban buses due to inability to depart from the bus stop after passenger service

Test site (bus stop)	Average delays incurred by urban buses due to the inability to depart from the passenger service area $\bar{d}_{z2\_m}$ (s/veh)				Probability of delays incurred by urban buses as a result of the inability to depart from the stop after ending passenger service P_{dz2_m} (%)			
	Measurement	Simulation			Measurement	Simulation		
		Min.	Mean	Max.		Min.	Mean	Max.
KRAK-01	12.3	11.1	13.1	15.3	25.0	22.5	27.5	32.5
KRAK-02	11.7	10.0	12.3	14.5	9.6	7.7	11.5	15.4
KRAK-03	11.6	9.8	12.0	14.0	10.3	7.7	12.8	17.9
KRAK-04	12.3	7.8	9.4	11.7	5.9	0	5.9	8.8
KRAK-05	14.7	13.2	15.6	17.4	5.6	0	8.3	13.9
KRAK-051	5.0	4.0	6.4	8.2	8.8	5.9	11.8	17.6
KRAK-06	7.1	5.9	8.2	10.1	20.7	17.2	20.7	27.6
KRAK-07	11.1	10.2	12.6	14.9	4.5	0	9.1	13.6
KRAK-08	6.8	5.2	7.6	9.8	10.0	0	13.3	16.7
KRAK-09	10.6	8.2	10.5	12.7	8.9	6.7	11.1	13.3
KRAK-091	4.9	1.8	3.7	6.3	15.9	13.6	18.2	20.5
KIEL-01	5.0	5.1	6.3	7.5	10.0	0	10.0	15.0
KIEL-02	8.5	6.9	9.2	11.7	19.0	0	23.8	28.6
KIEL-03	36.0	29.8	32.2	34.5	68.8	62.5	68.8	81.3
KIEL-04	0	0	1.1	3.0	0	0	7.1	14.3
KIEL-05	0	0	0	0	0	0	0	0
KIEL-06	0	0	0	0	0	0	0	0
KIEL-07	8	5.1	9.1	11.0	5.0	0	5.0	15.0
KIEL-08	0	0	0	0	0	0	0	0
KIEL-09	0	0	1.1	2.0	0	0	8.3	16.7
KIEL-10	0	0	1.5	3.5	0	0	6.7	13.3
KIEL-11	5.0	5.1	6.1	6.9	4.9	0	4.9	4.9
KIEL-12	7.5	2.9	6.0	9.1	2.8	0	3.1	6.0
KIEL-13	2.0	0.9	2.5	5.9	3.5	0	3.5	8.4
KIEL-14	3.0	1.1	4.1	7.2	4.2	0	5.1	9.1

Table C.4. Comparison of simulated and measured average delays of suburban and intercity buses due to inability to depart from the bus stop after passenger service

Test site (bus stop)	Average delays incurred by suburban and intercity buses due to the inability to depart from the passenger service area $\overline{d}_{z2\_z}$ (s/bus)				Probability of delays incurred by suburban and intercity buses as a result of the inability to depart from the stop after ending passenger service P_{dz2_z} (%)			
	Measurement	Simulation			Measurement	Simulation		
		Min.	Mean	Max.		Min.	Mean	Max.
KRAK-01	10.1	7.8	10.4	11.9	32.7	30.6	34.7	38.8
KRAK-02	12.7	8.7	11.0	12.4	22.0	17.1	19.5	26.8
KRAK-03	12.3	10.1	11.7	14.1	20.4	16.3	18.4	26.5
KRAK-04	11.8	9.5	11.2	13.0	21.7	20.3	23.2	24.6
KRAK-05	5.3	3.8	6.0	7.6	20.0	17.5	22.5	25.0
KRAK-051	6.8	3.8	5.9	7.4	28.6	27.0	28.6	33.3
KRAK-06	6.8	3.5	5.6	7.1	17.0	12.8	14.9	21.3
KRAK-07	6.0	5.4	7.1	8.5	4.5	3.0	6.1	9.1
KRAK-08	8.0	7.2	9.1	10.6	17.5	16.3	18.8	21.3
KRAK-09	13.3	10.5	12.4	13.5	43.1	38.9	41.7	47.2
KRAK-091	16.4	13.3	15.6	17.4	43.2	40.5	43.2	48.6
KIEL-01	1.0	0	1.5	3.0	5.6	2.8	8.3	11.1
KIEL-02	7.4	6.8	8.4	9.6	11.4	8.6	11.4	17.1
KIEL-03	29.1	29.5	31.4	33.8	48.3	41.4	48.3	55.2
KIEL-04	9.8	7.8	9.0	10.9	9.7	6.5	12.9	19.4
KIEL-05	0	0	1.4	2.5	0	0	5.0	15.0
KIEL-06	8.0	6.3	7.5	9.0	5.3	0	10.5	15.8
KIEL-07	9.0	7.5	8.6	9.1	15.4	0	7.7	23.1
KIEL-08	14.7	12.3	13.6	14.9	3.6	0	7.1	10.7
KIEL-09	0	0	1.1	2.3	0	0	7.7	15.4
KIEL-10	11.5	6.7	9.8	11.4	7.1	3.6	10.7	14.3
KIEL-11	2.0	1.0	2.6	3.5	7.4	0	3.7	7.4
KIEL-12	0	0	5.0	11.0	0	0	3.7	7.2
KIEL-13	12.0	0	7.0	13.1	11.1	0	12.5	37.5
KIEL-14	10.0	0	6.5	12.2	14.2	0	14.2	28.4

Table C.5. Comparison of simulated and measured additional average stopping time delays for taxis and other vehicles moving in the lane with a bus stop

Test site (bus stop)	Additional average stopping time delays for taxis and other vehicles moving in the lane with a bus stop $\overline{d}_{z\_tds}$ (s/veh)				Probability of additional delays for taxis and other vehicles moving in the lane with a bus stop P_{dz_tds} (%)			
	Measurement	Simulation			Measurement	Simulation		
		Min.	Mean	Max.		Min.	Mean	Max.
KRAK-01	16.7	15.5	16.3	18.5	25.0	20.0	22.5	27.5
KRAK-02	17.5	16.3	17.2	19.5	12.5	6.3	12.5	15.6
KRAK-03	13.7	11.7	12.7	14.6	18.2	15.2	19.7	21.2
KRAK-04	18.9	16.5	17.7	18.8	34.8	31.9	33.3	36.2
KRAK-05	10.8	8.4	11.4	11.9	15.0	5.0	10.0	20.0
KRAK-051	11.6	10	12.1	12.9	7.1	0	3.6	10.7
KRAK-06	24.0	23.3	25.4	26.5	25.0	0	12.5	25.0
KRAK-07	0	0	0	0	0	0	0	0
KRAK-08	14.9	11.4	13.0	14.6	36.4	18.2	27.3	36.4
KRAK-09	13.0	12.5	13.8	15.9	10.0	0	5.0	15.0
KRAK-091	28.7	28.9	29.4	31.4	3.3	0	3.3	6.7
KIEL-01	0	0	0	0	0	0	0	0

Test site (bus stop)	Additional average stopping time delays for taxis and other vehicles moving in the lane with a bus stop $\bar{d}_{z\_tds}$ (s/veh)				Probability of additional delays for taxis and other vehicles moving in the lane with a bus stop P_{dz_tds} (%)			
	Measure-ment	Simulation			Measure-ment	Simulation		
		Min.	Mean	Max.		Min.	Mean	Max.
KIEL-02	0	0	0	0	0	0	0	0
KIEL-03	33.3	32.6	34.3	35.5	20.8	18.8	20.8	22.9
KIEL-04	11.7	9.7	10.9	13.0	10.9	10.1	10.5	11.3
KIEL-05	13.0	11.4	12.2	14.2	57.1	28.6	42.9	71.4
KIEL-06	2.0	1.2	2.5	3.6	2.1	0	2.1	4.3
KIEL-07	21.0	18.1	20.1	20.7	14.3	0	14.3	28.6
KIEL-08	0	0	0	0	0	0	0	0
KIEL-09	20.0	9.4	21.5	22.8	50.0	0	50.0	100.0
KIEL-10	9.0	9.1	10.2	11.1	15.0	5.0	10.0	20.0
KIEL-11	0	0	0	0	0	0	0	0
KIEL-12	0	0	0	0	0	0	0	0
KIEL-13	0	0	0	0	0	0	0	0
KIEL-14	0	0	0	0	0	0	0	0

Table C.6. Comparison of simulated and measured additional average stopping time delays for suburban and intercity buses moving in the lane with a bus stop

Test site (bus stop)	Additional average stopping time delays for suburban and intercity buses moving in the lane with a bus stop $\bar{d}_{z\_z}$ (s/veh)				Probability of additional delays for suburban and intercity buses moving in the lane with a bus stop P_{dz_z} (%)			
	Measure-ment	Simulation			Measure-ment	Simulation		
		Min.	Mean	Max.		Min.	Mean	Max.
KRAK-01	13.0	12.5	14.1	14.8	60.0	56.0	60.0	68.0
KRAK-02	13.8	10.4	12.8	13.5	38.6	34.1	38.6	43.2
KRAK-03	13.7	12.6	14.4	14.9	63.6	60.6	66.7	69.7
KRAK-04	18.5	17.5	19.3	20.5	50.0	46.2	53.8	57.7
KRAK-05	10.9	8.8	9.6	11	51.5	48.5	54.5	57.6
KRAK-051	13.2	12.9	14.2	14.9	57.1	50.0	64.3	71.4
KRAK-06	6.0	6.7	7.0	8.5	14.3	10.7	17.9	21.4
KRAK-07	0	0	0	0	0	0	0	0
KRAK-08	10.2	9.8	11.4	12.8	40.0	30.0	50.0	60.0
KRAK-09	14.8	13.3	14.1	15.5	33.3	29.2	37.5	41.7
KRAK-091	18.0	15.7	17.1	18.1	14.8	11.1	18.5	22.2
KIEL-01	0	0	0	0	0	0	0	0
KIEL-02	0	0	0	0	0	0	0	0
KIEL-03	4.0	5.0	6.0	7.0	50.0	0	50.0	100.0
KIEL-04	5.0	3.0	3.9	6.0	20.0	0	40.0	60.0
KIEL-05	6.0	6.0	6.9	8.0	75.0	50.0	75.0	100.0
KIEL-06	0	0	0	0	0	0	0	0
KIEL-07	5.8	5.5	6.6	7.3	62.5	50.0	75.0	87.5
KIEL-08	0	0	0	0	0	0	0	0
KIEL-09	15.0	13.1	14.1	15.5	16.7	8.3	16.7	33.3
KIEL-10	11.0	8.0	9.0	10.5	25.0	0	50.0	75.0
KIEL-11	5.0	3.0	3.9	6.0	3.8	0	3.8	7.6
KIEL-12	3.2	0	4.5	8.0	4.1	0	4.6	7.2
KIEL-13	4.0	0	5.6	9.9	5.1	0	5.5	8.0
KIEL-14	2.6	0	3.3	7.1	3.6	0	4.6	9.1

Table C.7. Comparison of simulated and measured additional average delays for vehicles in adjacent lanes due to buses and other vehicles re-entering the traffic stream from bus stops

Test site (bus stop)	**Additional average stopping time delays for vehicles in adjacent lanes $\overline{d}_{z\_ps}$ (s/veh)**				**Probability of additional delays for vehicles in adjacent lanes P_{dz_ps} (%)**			
	Measure-ment	**Simulation**			**Measure-ment**	**Simulation**		
		Min.	**Mean**	**Max.**		**Min.**	**Mean**	**Max.**
KRAK-01	6.3	6.1	7.1	8.3	14.1	12.2	13.1	14.9
KRAK-02	3.4	1.9	3.3	4.1	1.3	1.0	1.1	1.6
KRAK-03	7.5	7.4	8.6	9.3	1.8	1.5	1.6	2.0
KRAK-04	4.8	5.1	5.4	6.0	2.1	1.6	1.8	2.4
KRAK-05	3.3	3.2	4.3	4.8	1.3	0.9	1.0	1.5
KRAK-051	8.6	7.1	7.6	8.8	2.1	1.7	1.8	2.4
KRAK-06	6.3	6.2	7.1	7.7	2.0	1.7	1.8	2.3
KRAK-07	0	0	0	0	0	0	0	0
KRAK-08	2.8	2.7	3.4	4.2	0.9	0.4	0.6	1.2
KRAK-09	4.6	4.4	5.1	5.5	4.2	3.7	3.9	4.5
KRAK-091	4.3	3.5	3.8	4.5	1.7	1.3	1.4	2.0
KIEL-01	4.8	4.7	5.4	5.9	3.7	2.9	3.2	4.1
KIEL-02	4.0	3.9	5.0	5.5	2.2	1.2	1.6	2.8
KIEL-03	3.1	2.9	4.0	4.3	12.5	11.9	12.1	12.8
KIEL-04	0	0	0	0	0	0	0	0
KIEL-05	2.0	1.7	2.6	3.4	0.5	0	0.2	0.9
KIEL-06	7.0	5.3	6.1	7.1	2.4	1.9	2.0	2.8
KIEL-07	5.0	4.1	4.5	5.0	1.5	1.0	1.2	1.8
KIEL-08	2.0	1.7	2.2	2.5	0.9	0.2	0.5	1.4
KIEL-09	2.0	1.2	1.5	2.1	0.6	0.6	0.3	0.9
KIEL-10	5.3	4.1	4.6	4.9	1.9	1.4	1.6	2.2
KIEL-11	2.0	1.8	2.5	3.1	0.5	0	0.5	1.0
KIEL-12	3.0	1.9	3.2	4.0	0.7	0	0.8	1.5
KIEL-13	4.0	2.2	4.5	4.8	0.6	0	0.7	1.6
KIEL-14	2.5	1.9	3.0	4.2	1.0	0	1.0	2.1